Synthesis and Thermal Analytical Screening of Metal Complexes as Potential Novel Fire Retardants in Polyamide 6.6

Alistair F. Holdsworth[1a], A. Richard Horrocks[1b] and Baljinder K. Kandola[1]

Affiliations: 1) – School of Engineering, University of Bolton, Deane Road, Bolton, BL3 5AB, UK, a) Now at School of Physical Sciences and Computing, University of Central Lancashire, Preston, UK b) Corresponding Author

Abstract

The development of new flame retardants is of ever increasing importance because of ecotoxicity concerns over existing systems and related regulatory pressures. From a range of low-toxicity, water-insoluble reagents, a total of 151 metal complexes were assessed for their potential to impart flame retardant behaviour in polymer matrices. These were successfully synthesised on a small scale and possible interactions were explored with a model engineering polymer, namely polyamide 6.6 (PA66). Powder mixtures of each complex with PA66 in a 1:3 mass ratio were analysed under air using TGA/DTA. Based on the stability of each at the typical processing temperature of 290 ^{o}C and its char forming potential (the final residue requirement at 580 ^{o}C being > 25%), selected mixtures were then analysed further using a differential mass loss technique. Metal complex/PA66 mixtures in which the differential residual mass at 470 ^{o}C was > 10% with respect to the theoretical value were considered to have a positive char forming interaction. Only eight of the metal complexes passed this last criterion including aluminium, tin (II) and zinc tungstates, three tin (II) phosphorus oxyanion complexes, iron (II) aluminate and iron (III) hypophosphite. These selected compounds were synthesised on a larger scale (c.a. 100 g), characterised and compounded into PA66 at 5 wt% for flammability assessment using LOI, UL94 and cone calorimetry. Of these, only aluminium tungstate and iron (II) aluminate showed some degree of FR behaviour with LOI values ≥ 23.0 vol% compared with PA66 (LOI = 22.9 vol%) and the former almost achieved a UL94 V-2 rating. However, while up to 32% reductions in total heat releases and up to 49% reduction in PHRR in cone calorimetric tests were observed for the metal complex/PA66 composites generally, those for $Al_2(WO_4)_3$ were 6 and 29% respectively and for $Fe(AlO_2)_2$ were 18 and 45% respectively

Keywords: metal complex, synthesis, polyamide 6.6, thermal analysis, char promotion, flammability

1.0 Introduction

The fire hazard posed by many polymeric materials often necessitates the incorporation of flame retardant compounds in order to meet stringent regulatory factors which increase safety with respect to ignition resistance or burning intensity.[1, 2] Recently, the replacement of potentially toxic flame retardant compounds and synergists such as certain monomeric polybrominated flame retardant/antimony trioxide

(ATO) formulations is of increasing importance and a significant amount of research continues to be devoted to this end.[3-6]

Many metal oxides possess a degree of flame retardant activity either on their own or in combination with other, primary flame retardants (FRs), the mechanism of action being dependent on the nature of metal centre present, the host polymer, and the interactions with any primary FRs present.[1, 7, 8] Metal hydroxides such as $Al(OH)_3$ and $Mg(OH)_2$ are known to have such a retardant effect through endothermic decomposition, releasing water into the vapour phase which subsequently dilutes the fire gases, and through the physical replacement of flammable material, although they are often required in high loadings (c.a. 50 wt%).[1, 2, 9, 10] Many metal oxides such as ZnO, Fe_2O_3 and SnO can provide an inherent degree of flame retardancy in some polymers,[7, 9, 11] while others, such as antimony trioxide, Sb_2O_3 (ATO), zinc hydroxystannate, (ZHS) and zinc stannate ($ZnSnO_3$, or $ZnSn(OH)_6$ (ZS) can act in concert with phosphorus or halogen flame retardants,[8, 9, 12-19] and, in the case of the last example, can additionally display smoke suppression activity.[14, 15]

Many inorganic synergists, however, display little or no interaction with their host polymer due to their chemical inertness, lack of viable reaction pathway with their host polymer or specific reaction mechanism with any primary flame retardant present.[16, 20] Neither ATO nor ZnS alone has any significant effect on the thermal degradation or flame retardant behaviour of most polymers, but in combination with an appropriate primary halogen-containing FR, a significant increase in performance is observed relative to a halogen-only control.[9, 14, 21] Both these synergists are understood to react with the hydrohalic acids (either HCl or HBr) produced by halogenated flame retardants during their thermal degradation to form volatile metal halides which serve to mediate the release of halogen radicals in the vapour phase.[9, 14, 21] For ATO, this processes is understood to take place via the gradual volatilisation of SbX_3 (where X is Cl or Br) from a range of antimony oxyhalides, whereas for ZnS, the process is less well understood, as either Zn or Sn could potentially be released to the vapour phase in the form of Zn (II), Sn (IV) or Sn (II) chlorides or bromides. With regard to zinc hydroxystannate in particular, Kicko-Walczak[22] has proposed that SnO, formed from

the degradation of ZnS or interaction with BrFRs, has a role in the flame retarding activity via the reaction:

$SnBr_2 + H_2O \rightarrow SnO + 2HBr$

It has been suggested by Cusack and coworkers[23] that SnO demonstrates vapour phase activity via hydrogen radical scavenging reactions such as:

$SnO + H^{\cdot} \rightarrow SnOH$

In contrast, we have recently demonstrated the potential of ZnO (formed from the thermal decomposition of ZnC_2O_4) to act as a condensed-phase char promoter in PA66 and as a promising synergist with bromine-containing retardants (BrFRs). [7]

In combination with phosphorus-containing flame retardants (PFRs), metal oxides generally act in the condensed-phase to form more coherent (glassy) barriers through their interaction with released H_3PO_4 to form metal phosphates, although this is by no means exclusive.[24] Synergists known to act with polymeric flame retardants include zinc borate and nitrogen-containing moieties, with the former forming phosphates and the latter reacting with these phosphates to form so-called P-O-N glasses.[9]

In this work and based on our previous study,[7] we demonstrate the methodology behind the selection, synthesis, screening and testing of more than 240 inorganic complexes for assessment as potential flame retardants and/or synergists for engineering polymers, exemplified by polyamide 66 (PA66). PA66 was selected for this study because of its use in electrical components requiring the combination of mechanical and flame retardant properties and is of interest to our sponsor. The overall screening process developed may be summarised in the following scheme:

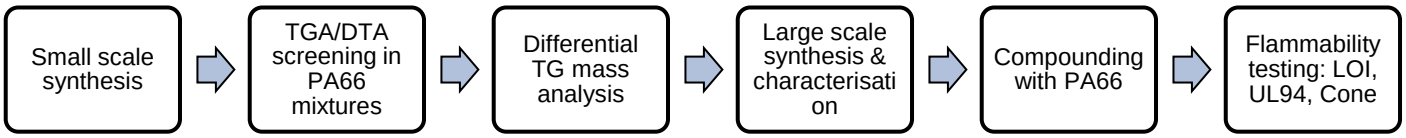

Scheme 1. A representation of the overall screening process.

In this scheme metal complex candidates are synthesised at a small scale to allow their screening for possible char-forming behaviour in mixtures with PA66 by TGA/DTA and differential TG mass analysis. The best forming candidates are synthesised at a larger scale, characterised and compounded in PA66, which samples are then subjected to flammability testing and then final selection.

Complexes were selected for their potential low toxicity and water insolubility, based on their general chemical properties. A 1:3 mass ratio of complex to PA66 was used for screening purposes as this represents the highest level of FR that would be incorporated into an engineering polymer, and the normally low-levels of flame retardant activity imparted by oxides would be amplified by the higher loadings. The potential of the produced complexes for introducing a degree of inherent condensed-phase FR activity into PA66 (in the form of char promotion) is also reported.

2.0 Experimental.

2.1 Materials

The selection of metal cations and complex metal-containing anions was based on the observation that oxy-compounds (often as mixed metal oxides) can act in a number of possible ways when heated in polymer matrices. [7, 8] Such reactions may include condensed-phase Lewis-acidic characteristics acting to cross-link oxygen- or nitrogen-containing polymers and/or as synergists with other primary phosphorus and/or bromine flame retardants.[2, 9] Some nitrogen-containing complex anions were also selected because it was postulated that they might release NO_x radicals that might act in a similar manner to the PO· radical in the vapour phase as a radical quenching agent.[9, 20] In a similar manner, P-containing compounds were

chosen for the potential ability to release radical-quenching $PO^{\cdot}$ radicals during polymer degradation as well as acting as Lewis acids to cross-link degrading polymers. [9, 20, 25]

As a consequence, the following compounds metal salts were acquired as cation sources: $MgCl_2.6H_2O$, $Al(NO_3)_3.9H_2O$, $CaCl_2.6H_2O$, $MnCl_2.4H_2O$, $FeCl_2.4H_2O$, $FeCl_3$, $CuCl_2.2H_2O$, $ZnCl_2$, $SnCl_2$, and $SnCl_4.5H_2O$. The following anionic species were obtained as sodium, potassium or ammonium salts , or as free acids which were deprotonated to the required level later stoichiometrically with sodium carbonate: $B(OH)_4^-$, CO_3^{2-}, $C_2O_4^{2-}$, NO_2^-, HO^-, $Al(OH)_4^-$, $Si(OH)_4^{2-}$, $H_2PO_2^-$, $H_2PO_3^-$, HPO_3^-, PO_4^{3-}, $P_2O_7^{4-}$, $P_3O_{10}^{5-}$, $PhPO_3^{2-}$, MoO_4^{2-}, SnO_3^{2-}, WO_4^{2-}, dimethylglyoxime (dmg), salicylaldoxime (sal) and 2-nitrophenol.

Based on the above simple and complex salts, Table 1 shows the cations and anions with the latter sub-divided into a number of groups based upon functionality (and likely mechanisms of action), namely oxides/oxyanions and N-containing and P-containing anions. These sub-groupings are used throughout the rest of this publication. All reagents were of reagent grade (≥98%) and procured from a range of suppliers including Sigma Aldrich, VWR International and Fisher.

100% polyamide 6.6 (PA66) was acquired from Invista Engineering polymers and used as procured (compounding grade, 100% PA66, MPt 260 ^oC, MFI 19.56 g/min @ 280 ^oC).

2.2 Synthesis of metal complexes

2.2.1 Small-scale syntheses

In order to undertake a potentially large (> 200) number of syntheses based on cations and anions in Table 1, a series of experimental matrices was prepared, whereby each cation would be reacted with each anion to determine whether the desired product precipitated in the first instance. Some reactions were selectively excluded as the anticipated complexes were already known to exhibit a degree of flame retardancy or to give water soluble products, and/or are commercially available as flame retardants. Section 3.1 presents these matrices with exclusions noted accordingly.

Each of the precursor compounds was first prepared as a 1 M standard solution in water (except $P_2O_7^{4-}$

and $P_3O_{10}^{5-}$ (0.5 M) and salicylaldoxime (0.1 M) due to limited solubility), from which complexes were prepared. Each compound was synthesised by a straightforward acid-base (cation-anion) precipitation reaction in which an amount of each cation solution was reacted stoichiometrically with the relevant anion solution so as to produce a charge-neutral complex or salt with a total liquor volume of 50 ml (except cases where lower concentration solutions were used). For example, the addition of Fe^{2+} as the chloride to MoO_4^{2-} as the sodium salt would involve the use of 25 ml of both solutions, whereas the addition of Sn^{4+} as the chloride to $Al(OH)_4^-$ as the sodium salt would use 10 ml of the former and 40 ml of the latter. The exception to this were the dimethylglyoximate (dmg^-) and salicylaldoximate (sal^-) complexes, which form planar species coordinating the metal centre with capping water and/or hydroxide ligands, as shown in Scheme 2 below, and as such these were always reacted with the metal ion in a 1:2 ratio.

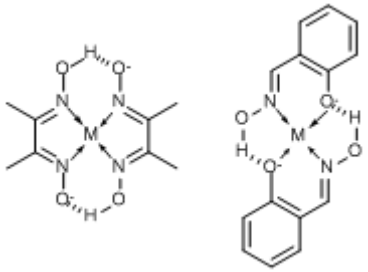

Scheme 2: Coordination of metal centres (M) with dmg^- (left) and sal^- (right)

Each acid/metal solution was added drop-wise to the base/cation solution, with stirring, over a period of about 10 min, followed by stirring for 30 min to allow the reaction mixture to complete. If no precipitate formed, the mixture was gently heated to boiling with stirring and then cooled to room temperature. In all reactions where a precipitate formed, the solid was isolated using Buchner filtration, washed several times with distilled water (200 ml) and then oven-dried overnight at 80 ^oC. Any changes in colour or other observations during the course of preparation were noted.

A cursory characterisation was carried out using X-Ray Fluorescence (XRF) or SEM/EDAX analysis of several complexes to assure the validity of the synthetic methodology. This selective methodology was justified by the results of the full characterisations of the 8 samples selected for larger scale synthesis (see Section 2.2.2 below).

2.2.2 Larger scale syntheses and characterisation

The initial small scale syntheses were designed using a readily-scaled batch precipitation method[26] which is used on an industrial level to produce numerous compounds, so that later, larger scale synthesis could be conducted for more thorough fire tests and to allow for a comprehensive characterisation to be undertaken. For the complexes selected for larger scale synthesis, again a similar method was used, for which the reaction conditions are shown in Table 2. For each target compound (A), the cation source (B, C g, D mol) was dissolved in water (E ml). Separately, the anion source (F, G g, H mol) was dissolved in water (I ml). The cation solution was then added dropwise to the anion solution with stirring over about 30 minutes and the resultant precipitate allowed to mature for a further 30 minutes. The product was then isolated by Buchner filtration, washed with an excess of water and dried under vacuum at 80 ^{o}C overnight. The reaction yield (J, %) was noted as were any observations through the course of the reaction. Reactions were scaled to give approximately 100 g of dry, hydrated product.

Various methods were employed for the characterisation of the produced metal complexes. X-Ray Powder Diffraction (PXRD) was conducted using a Brucker D8 diffractometer with a copper kα radiation source with facilities kindly provided by the University of Manchester. XRD patterns were converted using PowDLL.[27] Elemental analysis was conducted using Atomic Absorption spectroscopy (AA) using a Perkin-Elmer Analyst 300, X-Ray Fluorecense (XRF) analysis was conducted using a PANalytical Axios analyser on loose and pressed powders, and Inductively-Coupled Plasma (ICP) spectroscopy was conducted using either a Thermo Scientific iCAP6300 or iCAP6000, all kindly provided by William Blythe Ltd. Tungsten content of several samples was determined gravimetrically (as WO_3) following the leaching of any cations using concentrated HCl. Particle Size Distribution (PSD) was conducted using a Malvern Hydro 2000MV analyser, kindly provided by William Blythe Ltd. Fourier-Transform Infra-Red Spectroscopy was performed using a Thermo-Scientific Nicolet iS10 analyser. Chloride analysis was conducted using a SevenCompact pH/IOh Cl^- selective electrode on 1 g of solid boiled in 100 ml of deionised water, kindly provided by William Blythe Ltd. All relevant detailed characterisation data can be found elsewhere [28].

Before the metal complexes could be compounded into PA66 via melt-blending (see Section 2.4), they were first calcined to remove any hydrating water molecules (Table 3). The temperatures of these were determined using the TGA responses of each compound. $SnWO_4$ was dried under vacuum to suppress oxidation.

2.3 Preparation of Powdered PA66 and PA66/Complex Powder Mixtures

The PA66 as procured was in the form of pellets, which were pulverised by first cooling them to -196 ^oC using liquid nitrogen before mechanically grinding them using a coffee grinder. This process was repeated several times until a sufficiently fine powder size was obtained which was then passed through a 50 µm sieve to ensure no larger particles remained. The powder was then dried at 80 ^oC before being used for TGA analysis in mixtures with each dried metal complex sample.

It was assumed that if any of the synthesised metal complexes possessed significant char-forming character in the presence of PA66, this would be observable if mixtures of PA66 and each complex in a mass ratio of 3:1 were studied by TGA/DTA in air. This ratio reflected the generally accepted commercial view that the maximum allowable flame retardant present in any engineering polymer is no greater than about 25wt% if serious loss of mechanical properties is to be avoided. Such mixtures were prepared by the addition of 30 mg of powdered PA66 and 10 mg of each powdered complex to a glass vial followed by intensive mechanical agitation. It should also be noted that PA66 melts at about 265 ^oC during the TGA/DTA analysis and as such, the mixed powders would form a finely divided suspension in the molten polymer. Duplicate results across several samples confirmed the efficacy of mixing.

2.4 Compounding of PA66/metal complex samples for flammability testing

Compounding of all PA66 formulations was undertaken using a laboratory-scale Thermo-Scientific twin-screw extruder. The six barrel heating elements were set at 250, 255, 260, 265, 270 and 275 ^oC respectively and a screw speed of 350 rpm was used. Prior to compounding, all PA66 polymer pellets and previously calcined flame retardant powders were dried at 80 ^oC for at least 36 h before processing (Table 3). Dry

compounded pellets were pressed into plaques (170 x 170 x 3 mm) using a hot press at 260 ^{o}C with a pressure of 20 kg/cm^2, followed by cutting into strips 12.7 mm wide for UL94 and LOI testing and 75 x 75 mm plaques for cone calorimetry analysis where appropriate. Levels of metal complex introduced were generally 5wt% with some being increased to 10wt%. These levels were lower than that used in the mixtures for TGA experiments in Section 2.3 to reflect the more common commercially used levels of inorganic flame retardants such as zinc stannate where cost must be considered in addition to potential flame retardant efficiency.[16]

2.5 Simultaneous Thermogravimetric/Differential Thermal Analysis (TGA/DTA)

All TGA/DTA experiments were performed using a TA Instruments SDT 2960 Simultaneous Thermogravimetric/Differential Thermal analyser with samples contained in platinum crucibles. 10 mg sample masses were heated at 20 ^{o}C/min from ambient temperature to 600 ^{o}C, under a flow of air at 100 ml/min. Air was selected as the atmospheric medium because the char-forming process for PA66 is promoted by the presence of air above 450^{o}C [14].

Further to the analysis of the PA66/complex powder mixtures, additional TGA/DTG analyses of the pure PA66 powder and each complex were recorded. This allowed for differential mass analysis calculations to be conducted in order to compare more clearly the temperature effect of each PA66/complex degradation process with a theoretical degradation curve for each mixture in which no interaction occurred.[29] For each temperature point, the differential mass (as a percentage of starting total mass) was calculated using Equation 1:

$$(1) \qquad (M_{diff})_T = (M_{PA66+complex})_T - ((0.75.M_{PA66})_T + (0.25.M_{complex})_T)$$

Where $(M_{diff})_T$ is the percentage mass difference between experimental and calculated, $(M_{PA66+complex})_T$ is the percentage mass of the PA66/complex mixture, $(M_{PA66})_T$ is the percentage mass of PA66 powder and $(M_{complex})_T$ is the percentage mass of the complex at a given temperature, T. All values of M are in % of starting mass at the same temperature point. Values were typically calculated every 20 ^{o}C between 300

and 580 ^{o}C. This method has been previously reported, but is explained in far greater detail below in Section 3.3.[7]

2.6 Flammability testing

Compounded PA66 samples were assessed for Limiting Oxygen Index (LOI) according to ASTM 2863, and UL-94 in the vertical orientation, according to ISO 1210. Cone calorimetry was also performed on samples which produced viable plaques using a 50 kW/m^2 heat flux (FTT cone calorimeter, Fire Testing Technology, UK) according to ISO 5660. Several parameters were determined, namely the times- to-ignition, T_{ig}, time-to-flame-out, T_{fo}, time-to-peak heat release rate, T_{PHRR}, the peak heat release rate, PHHR, and total heat release rate, THR. This enabled the potential reducing effects that addition of metal complexes (MC) to PA66 had on PHRR and THR values to be recorded as respective percentage reductions of each parameter with respect to PA66 control values as R_{PHRR} (= (1-($PHRR_{PA66 + MC}$/$PHRR_{PA66}$))x100) and R_{THR} (= (1-($THR_{PA66 + MC}$/THR_{PA66}))x100).

3.0 Results and Discussion

3.1 Small-Scale Synthesis of Metal Complexes

The matrix in Table 4 highlights the reactions that were undertaken to prepare the metal complexes, grouped by anion functionality. Each cell contains the ratio of metal to anion used. Additionally, any cells coloured red failed to precipitate a product. Cells coloured blue are known (patented or commercially available) existing FR species and were thus not prepared and cells coloured green contain the same metal in both cation and anion, and again were not synthesised as single metal oxides are more readily produced by other means. It should be noted that the carbonates and hydroxides generally decompose upon drying to their respective metal oxides via loss of CO_2 or H_2O respectively.

Out of the potential 209 compounds, 142 were successfully isolated and thus a ready screening method for possible interactions with the chosen model engineering polymer, PA66, was required. We have previously

reported the screening and testing of divalent metal oxalate salts,[7] but these results are included here for completeness. Samples in the blue cells in Table 4 are all known to be flame retardants and in fact aluminium hypophosphite is patented and commercially available[30, 31]. They have been included above to present the complete matrix, but have been excluded from further study.

All metal complexes that were successfully isolated were analysed as a 1:3 powder mixture with PA66 using TGA/DTA to determine the effect of each compound on the degradation of PA66.[3]

3.2 TGA/DTA Screening of Metal Complexes for Interactions with PA66

In order to determine which of the produced metal complexes were most suitable for further study, a number of screening parameters were devised based upon favourable processing and fire retardancy observations.[3, 28] These parameters were:

i. T_5 – Temperature to 5% mass loss (^oC), which should have a minimum value of 200 ^oC, excluding hydrated compounds, thereby indicating a generally high level of thermal stability in PA66.
ii. T_{10} – Temperature to 10% mass loss (^oC), which should have a minimum value of 300 ^oC, excluding hydrated compounds, thereby indicating acceptable thermal stability when in molten PA66 above a typical melt processing temperature for PA66 formulations.
iii. T_{50} – Temperature to 50% mass loss (^oC), which should have a minimum value of 350 ^oC and thus be a further indicator of potential stability in molten PA66 and of onset of primary degradation processes.
iv. M_{580} – Mass remaining (%) at 580 ^oC in air, with a minimum value of 25%. Each mixture contains 25 wt% of a metal complex, and thus any residue above this level would represent an increase in metal-sensitised char promotion relative to pure PA66, and a degree of stability of this char to high temperature in air.
v. Absence of significant DTG peaks under 350 ^oC which would suggest an absence of endothermic degradation reactions accompanied by mass loss.

vi. DTA peak character such as their correspondence with DTG peaks and absence of any significant endo- or exothermic degradative behaviour below 350°C apart from the PA66 melting endotherm.

Exemplar TGA and DTA data highlighting the interpretation of each factor are presented in Figures 1 and 2 respectively, showing the degradation of pure PA66 powder, a PA66/$ZnWO_4$ mixture and $ZnWO_4$ powder.

The TGA response for pure PA66 shows the presence of the oxygen-sensitised shoulder of increased char formation at 450°C and respective DTG maximum reported by us previously [14] which by 580°C reduced to zero, hence the selection of this temperature for determining residual masses of PA66/metal complex mixtures. The slight mass losses for both PA66-containing samples at < 100 °C are due to the loss of adsorbed water, and the 10% mass loss for pure $ZnWO_4$ corresponds to dehydration of the synthesised, dried (at 80°C) $ZnWO_4.2H_2O$ to the anhydrous analogue. Between 100 and about 350 °C very little further mass losses are seen for all three samples, but at about 370°C both pure PA66 and PA66/$ZnWO_4$ start to undergo thermal degradation with the generation of volatiles. For PA66, this continues via a two-step degradation process until no mass remains at about 580 °C, in agreement with the literature.[32] However, PA66/$ZnWO_4$ undergoes a three-step degradation process, giving a much higher residue than the 25% mixture content of $ZnWO_4$ would be expected to produce, due to the formation of oxidatively stable char. The nature of the reactions occurring between $ZnWO_4$ and PA66 over the 350-500°C range are not known and would require further research to elucidate, but for the purposes of this study, they are considered to be the precursor reactions for eventual char formation, which like that for PA66 alone, may be oxygen dependent [14]. Over the same temperature range (370-580°C) there is a very gradual reduction in the mass of zinc tungstate although > 85% remains at the higher temperature. This approximate 5% mass loss from the dehydrated product could be attributed to the sublimation of ZnO from $ZnWO_4$.[33]

In terms of effect on mass loss rates, DTG curves in Figure 1 suggest that $ZnWO_4$ accelerates the degradation of PA66 significantly by lowering the onset of degradation compared to the virgin polymer, but the carbonaceous part of the residue formed above about 400°C is relatively stable to oxidation in the range 500-600°C.

Examination of the respective DTA responses in Figure 2 shows that loss of moisture in each sample corresponds to the respective endotherms in the 100 ^{o}C region followed by the PA66 fusion endotherms at about 265^{o}C. At higher temperatures, the sensitising effect of $ZnWO_4$ on the degradation of PA66 is clearly seen as an increased endothermicity in the 350-400 ^{o}C region compared with a generally exothermic behaviour of PA66 above 350 ^{o}C in air. Furthermore, above 500 ^{o}C the mixture has a lower exothermic character than pure PA66 reflecting the relative thermal stability of the residue as noted from the TGA response. While no analysis of the residue above 500 ^{o}C has been undertaken, it is highly likely that it comprises both inorganic residues from zinc tungstate as well as carbonaceous char from the PA66. Of all the simple linear aliphatic polyamides, PA66 is noted for its greater tendency to cross-link when heated and form eventual char and that such cross-linking reactions are catalysed by variable oxidation state transition metals such as iron and copper.[32]

As many inorganic FRs do not display any significant interaction with their host polymer, any char resulting at high temperatures (T_{580}) was seen to be advantageous, and as such, this screening parameter was the primary measure of performance and determiner of suitability for further study, if all other parameters were met. The values of T_{580} of each metal complex/PA66 composition are reported in Table 5, with a value greater than or close to 25 wt% deemed to be favourable.

Table 5 lists the 17 complexes that met the 6 screening criteria outlined above and includes only the respective T_{580} values. In this respect, $Fe(Al(OH)_4)_2$ was a borderline case of interest to our sponsor (mass at T_{580} = 24.8%) and so was included for further study. The full table of respective criteria values recorded in this analysis can be found in reference 28. All borates were rejected at this stage including the marginal Mn^{2+} and Sn^{2+} borates in light of potential toxicity concerns.[34] Two carbonates (Sn^{2+} and Sn^{4+}) and one hydroxide (Fe^{3+}) were considered for further study. It should be noted that compounds such as these tend to decompose releasing either CO_2 or H_2O either during synthesis or when heated and as such should be considered as oxides of their relevant cations, rather than containing the anions listed. No oxalates, molybdates, stannates or pyrophosphates were considered for further study, although tin (IV) silicate,

three tungstates (Al^{3+}, Zn^{2+} and Sn^{2+}), several Fe^{3+} and Sn^{2+} phosphorus complexes and several phosphites were selected. A single nitroxy compound (tin (IV) hexanitritozincate) was also included, as this almost met the screening criteria (T_{580} = 24.4%) and was of interest as having a potentially novel vapour phase mechanism of action [20], whereas the better performing zinc (II) nitroxyphenolate was not as this had a deleterious effect on the degradation of PA66 at processing temperatures.

3.3 Differential Mass Analysis using TGA.

The 19 metal compounds selected for further study are outlined in Table 6. This number, however was still too large to warrant larger scale synthesis and detailed fire testing, and so, differential mass TGA was undertaken, as described in Section 2.4. The differential mass curve was created by subtracting the calculated, weighted average TGA response from the observed response between 300 and 580 ^{o}C. The suitability of each sample for scaling up to a larger synthesis following this analysis was determined by the following criteria:

(i) Additional char formation in the region 480 - 500^{o}C must be greater than or equal to 10%. Figure 2 shows that for pure PA66, this temperature range follows the point at which the first volatilisation stage ends and the formation of char occurs. The TGA residue levels at 580 ^{o}C for the PA66/metal complex mixtures reported in Table 4, however, comprise both inorganic and carbonaceous contents. Therefore, excess residues observed above 450 ^{o}C above the theoretical zero-interaction level calculated will be essentially carbonaceous char only reflecting the air-sensitised char formation occurring in PA66.[14] Table 6 lists the highest differential mass values for PA66/complex mixtures over the range 480-500^{o}C.

(ii) Additional char formation above 500 ^{o}C must be maintained between 540-560 ^{o}C. This represents the stability of the char to oxidation, which usually occurs above 450^{o}C and for pure PA66, char has been fully oxidised by 580^{o}C (Figure 1). Table 6 includes the highest differential mass values over 540-560 ^{o}C.

(iii) Sensitised PA66 volatilisation below 450 ^{o}C is reduced in the presence of metal complex. All PA66/complex mixtures show a negative mass difference region over an approximate 350-450 ^{o}C range, indicating significant interaction between PA66 and each complex. This suggests that reduced volatile formation occurs in addition to the observed increased char formation. The effect of this observation can be quantified by comparing the relative depth and extent of the observed differential mass minimum within this temperature range together with the TGA-derived T_{10} (onset of degradation) values listed in Table 6 for each PA66/complex mixtures

An exemplar representation of this process for a PA66/$ZnWO_4$ mixture, showing the difference between experimental and calculated TGA responses is shown in Figure 3, and in Table S1, which provides an example of the underlying numerical TGA data for PA66, $ZnWO_4$ and PA66/$ZnWO_4$ mixtures. As can be seen, $ZnWO_4$ promotes the formation of a significant amount of additional residue above 470 ^{o}C when compared to the calculated response. The minimum between 380 and 470 ^{o}C represents the acceleration in the volatilisation of PA66 by $ZnWO_4$ as discussed above. Table 6 shows that some reduction in T_{10} occurs (384 ^{o}C) relative to pure PA66 (409 ^{o}C). The depth and extent of this minimum in Figure 3 relates to the degree of interaction between and effect on the degradation of PA66 by the metal complex.

Table 6, below, outlines the effect of each metal complex on the degradation and char promotion of PA66 via ready comparison of the temperature to onset of degradation (T_{10}) and the observed differential mass values between 480-500 ^{o}C and 540-560 ^{o}C, representing the level of char promotion from the degradation of PA66 and the stability of that char to oxidation respectively. The values presented in Table 6 are discussed with selected graphs below.

Based on the results in Table 6 and the graphical representation in Figure 4 below, it can be seen that of the carbonates and hydroxides analysed, the SnO and SnO_2 derived from the latter both promote a large amount (> 10%) of char at 480 ^{o}C, with the former producing 19% above the expected amount. The stability of this char, however, was limited, degrading rapidly with temperature. $Fe(OH)_3$, or more likely, FeO(OH) only promoted a limited (7%) amount of additional char at elevated temperatures. With these

factors in mind, none of these samples was considered for further large scale study.

Only one aluminate ($Fe(Al(OH)_4)_2$) was studied using the differential mass TGA method, producing approximately 8 wt% of additional char which was sustained over 520 ^oC, combined with a relatively low effect on the degradation of PA66. At this stage, however, this compound was considered for further study due to sponsor interest.

Of the three tungstates analysed, namely $Al_2(WO_4)_3$, $ZnWO_4$ and $SnWO_4$ only the two last produced significant amounts (> 10 %) of additional char, which was stable at high temperatures (see Figure S1). However, although $Al_2(WO_4)_3$ generated only 9 % additional char at 540 ^oC, it was included for further large scale study. The mechanism of action of these compounds in promoting char could be attributed to a number of potential actions, including reductive or acid-catalysed cross-linking.[8, 35]

Iron (III) hypophosphite showed high levels of differential mass char promotion (16%) in PA66 over the whole 480-550 ^oC range and so was considered to be appropriate for further large scale study. This compound may display this behaviour as the P-H bonds of the hypophosphite anion are quite labile at high temperatures and capable of reacting with a range of organic moieties. Additionally, the anion is also a strong reducing agent, and thus could be capable of reductively cross-linking PA66. [30, 36, 37]

The high temperature differential masses recorded in Table 6 for the high char-forming iron (III) and tin (II) hydrogen phosphites (see also Figure S2) indicated that only the latter showed a char level > 10% and a lower minimum at about 440 ^oC, which is reflected by a relatively high T_{10} value (393 ^oC). The mechanism of char promotion is likely a combination of Sn^{2+} Lewis acidity and ionic reductive cross-linking of PA66.[35, 36]

Iron (III) hydrogen phosphite was rejected at this stage since the differential char value was < 10%.

Based on the thermal data for the Fe(III), Cu, Zn and Sn(II) phosphite complexes in PA66 in Table 6 (see also Figure S3) and in spite of high residues from the initial TGA studies of PA66/compound mixtures (see Table 5), zinc and tin (II) phosphites were rejected because additional char residues at 500 ^oC were less than 10% Iron (III) phosphite was rejected because of the rapid decrease in char at temperatures above 500 ^oC. Copper (II) phosphite, while giving the highest differential mass of all the phosphites at about 580 ^oC,

promoted the greatest PA66 degradation in the 350-450^{o}C region, which was reflected in the large minimum over the350-475^{o}C and low T_{10} value (330^{o}C), was also rejected.

Of the several other tin (II) compounds containing phosphorus-oxyanions, $SnPhPO_3$, $Sn_5(P_3O_{10})_2$ and $Sn_3(PO_4)$ were selected for differential mass studies, and, as seen in Table 6 (see also Figure S4), the first two demonstrate char levels ≥ 10% above 480 ^{o}C and quite shallow minima at about 440 ^{o}C, which were matched by quite high T_{10} values. These were included for further study while tin(II) phosphate was rejected due to differential residue above 500 ^{o}C < 10% and the large deleterious effect on the degradation of PA66, as represented by the broad and extensive minimum in the 350-475^{o}C region and low T_{10} value (356^{o}C).

Of all the nitrogen-containing complexes only the PA66/tin(IV) hexanitrozincate mixture was further evaluated using the differential mass method and, as a result of differential char levels at 500 ^{o}C < 5%, it was rejected.

Thus, the eight compounds selected for further study involving large scale synthesis and fire testing were:

- $Fe(Al(OH)_4)_2$ – Iron (II) aluminate
- $Al_2(WO_4)_3$ – aluminium tungstate
- $ZnWO_4$ – zinc tungstate
- $SnWO_4$ – tin (II) tungstate
- $Fe(H_2PO_2)_3$ – iron (III) hypophosphite
- $Sn(H_2PO_3)_2$ – tin (II) hydrogenphosphite
- $SnPhPO_3$ – tin (II) phenylphosphonate
- $Sn_5(P_3O_{10})_2$ – tin (II) triphosphate

3.4 Large Scale Synthesis and Characterisation

The syntheses of the eight selected metal complexes were scaled up to approximately 100 g scale (see **Section 2.2.2**) based upon simple inorganic precipitation processes [26] and a full characterisation of each

compound undertaken using a range of appropriate methods, outlined in Section 2.2.2. The full results of these are described elsewhere[28] and the particularly notable observations relevant to this paper are presented below and included in the supplementary information as Table S2. Of the eight compounds selected for scale-up, seven compounds were successfully prepared with tin (II) triphosphate proving to be difficult to isolate as a the stable precipitate form observed during small scale synthesis (see below).

Aluminium, Zinc and Tin (II) Tungstates

Aluminium, zinc and tin (II) tungstates ($Al_2(WO_4)_3$, $ZnWO_4$ and $SnWO_4$ respectively) were synthesised by the addition of stoichiometric amounts of the nitrate (Al) or chloride (Zn, Sn) salts to $Na_2WO_4.2H_2O$. In all three cases this resulted in the precipitation of the desired (hydrated) phase, although satisfactory XRD analysis could only be performed on material that had been calcined (800 ^oC for Al and Zn, 240 ^oC under vacuum for Sn) as the dried, hydrated material was amorphous. Each reaction produced the desired material.

Tin (II) Phosphite

Tin (II) phosphite ($SnHPO_3$) was synthesised by the addition of $SnCl_2$ to two equivalents of NaH_2PO_3. The initial synthesis target was the hydrogen phosphite, $Sn(H_2PO_3)_2$, although this latter may serve as an intermediate to the more stable compound produced. As shown by the SEM image, (Figure 5) this compound forms plate-like crystals. The observed XRD pattern and EDAX results match the reference pattern and elemental composition respectively. Interestingly, this compound is rather hydrophobic, as it was readily filtered and seemed to coagulate readily rather than settle as per other inorganic compounds. Additionally, it was easily incorporated into PA66 by melt blending at higher concentrations than other inorganic additives, described in further detail below.

Tin (II) Phenylphosphonate

Tin (II) phenylphosphonate ($SnPhPO_3$) was synthesised by the addition of $SnCl_2$ to one equivalent of Na_2PhPO_3. As shown by the SEM image, this compound forms plate-like crystals (see Figure S5), similar to

the related $SnHPO_3$ above. The XRD pattern of this compound also indicates the plate-like nature of the particles (Figure S6).[37] This compound was also rather hydrophobic, displaying similar behaviour to $SnHPO_3$ and was able to be incorporated into PA66 at a higher level by melt blending than other inorganic additives, described in further detail in Section 3.5.

Iron (II) Aluminate

Iron (II) aluminate was synthesised by the addition of stoichiometric amounts of $FeCl_2$ to $NaAl(OH)_4$. This compound initially formed a green-grey precipitate which changed colour rapidly to brick red over the course of the addition, suggesting oxidation of Fe (II) to Fe (III). XRD analysis indicated that the dried product was mostly $Al(OH)_3$ and mixed iron oxides. Upon calcination at 240 ^oC before compounding, this compound loses water to form a mixed Fe-Al oxide.

Iron (III) Hypophosphite

Iron (III) hypophosphite was synthesised by the addition of stoichiometric amounts of $FeCl_3$ to NaH_2PO_2, forming the desired phase.

Tin (II) Triphosphate

Attempts to synthesise tin (II) triphosphate on a larger scale resulted in the formation of a gelatinous phase not observed on the smaller scale and as such no viable product could be isolated. For this reason, this compound was not studied further.

3.5: Compounding and Flammability Testing

Each was compounded into PA66 alone at 5 wt% to determine compatibility via melt blending following calcination at up to 240 ^oC. No mass losses or phase changes were observed for any of the compounds in the processing temperature range of PA66 (250-275 ^oC), as measured by TGA. All compounds were successfully incorporated at this level, which is a reasonable maximum for an inorganic component in an

engineering polymer. Beyond this level, however, difficulties in processing become apparent, as attempts to incorporate $Al_2(WO_4)_3$ into PA66 at 7.5 wt%, for example, were met with failure due to thinning of the composite melt at processing temperatures. As noted above, $SnHPO_3$ and $SnPhPO_3$ displayed some interesting hydrophobic character during synthesis and as such were capable of being blended into PA66 at 10 wt%, with higher levels still possible, though these were not tested. Compounded PA66 sample containing each metal complex were then hot-pressed into plaques for flammability testing (see Section 2.6). Viable plaques were produced for all compounds except $Fe(H_2PO_2)_3$, which allowed only enough material for LOI and UL-94 tests to be performed. Fire performance was conducted using LOI, UL-94 and cone calorimetry, with the thermal stability of the samples determined using TGA/DTA under both air and nitrogen as for the previous small-scale complex/PA66 mixtures. These results are presented in Table 7 with cone calorimetry heat release values presented graphically in Figures 6a and 6b, with total heat release values presented in Figure 7. Please note that $SnHPO_3$ and $SnPhPO_3$ were tested separately from the other samples and as such there is a different control for the cone calorimetry, UL-94 and LOI for comparison.

Generally, as can be seen from Table 7 and Figures 6(a), 6(b) and 7, the eight tested metal complexes imparted limited flame retardant behaviour to PA66. With respect to the thermal stability of the PA66 control, TGA/DTA data under air shows a reduction in both onset (T_5) and peak degradation rate (DTG_{max}) temperatures when each metal complex is present. Based on the previous differential mass analyses in Section 3.3, apart from iron II aluminate, all residual mass percentages at 500 and 580 ^oC should be greater than those for the PA66 control, although in these previous experiments, metal complexes were present at 25 wt% levels. At the lower 5 wt% level, only $Al_2(WO_4)_3$, $Fe(H_2PO_2)_3$, $Sn(H_2PO_3)_2$ and $SnPhPO_3$, produced increased residues at both 500 and 580 ^oC whilst $SnWO_4$ did so at 500 ^oC only. Thermal analytical data under nitrogen shows that each metal complex present at 5 wt% or greater increases the percentage mass residues at 500^oC and above compared to the PA66 control although absolute respective values are lower in nitrogen than in oxygen suggesting that the char-formation process is oxygen sensitised

as noted previously.[14] The higher concentrations of $Sn(H_2PO_3)_2$ and $SnPhPO_3$ showed an increased effect on the char formation of the polymer as expected, indicating that at these levels and above, a degree of inherent fire performance may be eventually achievable.

With respect to the more basic fire tests undertaken (UL-94 and LOI), only a limited changes in performance were observed with only $Fe(AlO_2)_2$ and $Al_2(WO_4)_3$ increasing LOI values slightly. However, if any of the metal complexes have an effect on the PA66 molecular mass, these will influence the LOI values determined in addition to or in association with any flame retardant effects. That most metal complex/PA66 composites showed a reduction in LOI most probably as a consequence of cross-linking that precedes the increases in char formation reported above in Table 6, suggests that associated reductions in melt dripping are the cause. With regard to UL94 testing, no composite gave consistent ratings although two of the three specimens of aluminium tungstate gave improved ratings.

A greater effect was observed on the cone calorimetric performance of the PA66 composites in that while times-to-ignition were all reduced with respect to pure PA66, total burn times were increased by about 10-20%. For all composites PHRR values were reduced, with $Fe(AlO_2)_2$ and $SnPhPO_3$ (at 5 wt%) reduced by about 45 and 29% respectively. Similarly, total heat release rates were reduced (Figure 8) with again these same composites showing reductions up to 32% compared to the control. Increasing the concentration of $SnHPO_3$ and $SnPhPO_3$ from 5 to 10% served to reduce the peak heat release rates further although no similarly consistent reductions in THR values were observed. In comparison with current commercial synergists, such as antimony III oxide and zinc stannate, similar effects are observed with respect to LOI and UL-94 and, while the two commercial compounds may lower the peak heat release rate of PA66 in cone calorimetry, they do not display the same reduction in total heat release observed for our metal complexes.[14]

4: Conclusions

We have described the small-scale synthesis, screening, scale-up and initial fire testing of a wide range of primarily metal complexes in PA66. These compounds were targeted as having the potential to impart a

degree of flame retardancy on their own into this representative engineering polymer determined by their propensity to generate char during TGA/DTA analysis. Of 142 starting compounds, 17 promising candidates were further analysed using the differential mass versus temperature technique to improve the ability to choose those most desirable for larger-scale fire testing. Of the 8 compounds selected for scale up, 7 were successfully produced at a larger scale and were able to be incorporated into PA66 at 5 or 10 wt% levels prior to their being subjected to a range of small scale fire tests. No significant improvements in LOI or UL94 performance were observed for the majority of tested compounds. Iron aluminate and aluminium tungstate did slightly improve the LOI of PA66, however, but only aluminium tungstate was able to produce evidence of its improving UL-94 performance. All the metal complexes lowered the peak heat release of PA66 during cone calorimetric analysis, with $Fe(AlO_2)_2$ and $SnPhPO_3$ both lowering PHRR by up to 45% and THR by up to 24 % compared to the pure PA66 control. However, while these compounds did not possess sufficient flame retardant activity to successfully inhibit the combustion of PA66 in their own right, they could be of interest as potential synergists in combination with other primary bromine- or phosphorus-containing primary flame retardants in a manner similar to antimony (III) oxide and zinc stannate. The high-throughput process of synthesis and screening presented here is considered by the authors to be a robust methodology for rapid determination of target species, although with suitable adaption to other analytical techniques, it could be applied to other fields. Although effective, a number of optimisations could be undertaken to improve the efficiency of the screening process, for example the use of high throughput flow synthesis in the preparation of similar compounds.[37, 38] The TGA/DTA testing methodologies used could be extended to the study of individual metal oxides (e.g. ZnO, SnO, SnO_2, WO_3, etc.) in addition to their combined mixed-metal compounds and by combining the TGA/DTA data with small-scale fire testing such as microcombustion calorimetry, their performance in combination with varying levels of different flame retardants could be rapidly assessed. The potential of the selected metal complexes as synergists with a number of flame retardants present in PA66 will be reported in a subsequent publication.

5.0 References:

1. Horrocks AR, Price D, editors. Flame retardant materials. Cambridge: Woodhead Publishing, 2001.
2. Weil ED, Levchik, Flame retardants for plastics and textiles. Munich: Carl Hanser Verlag, 2009
3. Papaspyrides CD, Kiliaris P, editors. Polymer green fire retardants. Amsterdam: Elsevier BV, 2014.
4. Murphy J. Flame retardants: trends and new developments. Plastics, Additives and Compounding 2001; 3(4): 16-20.
5. de Wit CA, Herzke D, Vorkamp K. Brominated flame retardants in the Arctic environment — trends and new candidates. Sci Total Environ 2010: 408(15); 2885-2918.
6. Law RJ, Alaee M, Allchin CR, Boon JP, Lebeuf M, Lepom P, Stern GA. Levels and trends of polybrominated diphenylethers and other brominated flame retardants in wildlife. Environ Int 2003:29(6); 757-770.
7. Holdsworth AF, Horrocks AR, Kandola BK, Price D. The potential of metal oxalates as novel flame retardants and synergists for engineering polymers. Polym Degrad Stab 2014; 110: 290-297.
8. Braun U, Schartel B, Fichera MA, Jager C. Flame retardancy mechanisms of aluminium phosphinate in combination with melamine polyphosphate and zinc borate in glass-fibre reinforced polyamide 6,6. Polym Degrad Stab 2007: 92; 1528-1545.
9. Laoutid F, Bonnaud M, Alexandre M, Lopez-Cuesta JM, Dubois P. New prospects in flame retardant polymer materials: from fundamentals to nanocomposites. Mater Sci Eng 2009: 63; 100-125.
10. Rothan R, Hornsby PR. Flame retardant fillers for polymers. In: Papaspyrides CD, Kiliaris P, editors. Polymer green fire retardants. Amsterdam: Elsevier BV, 2014. p. 289.
11. Rault F, Pleyber E, Campagne C, Rochery M, Giraud S, Bourbigot S, Devaux E. Effect of manganese nanoparticles on the mechanical, thermal and fire properties of propylene multifilament yarn. Polym Degrad Stab 2009: 94; 955-964.
12. Hastie JW. Molecular basis of flame inhibition. J Nat Res Bureau Stds 1973: 77A; 733-754.
13. Petsom A, Roengsumran S, Ariyaphatanakul A, Sangvanich P. An oxygen index evaluation of flammability for zinc stannate as synergistic flame retardants for acrylonitrile-butadiene-styrene copolymer. Polym Degrad Stab 2003: 80(1); 17-22.
14. Horrocks AR, Smart G, Kandola BK, Holdsworth AF, Price D. Zinc stannate interactions with flame retardants in polyamides; Part 1: Synergies with organobromine-containing flame retardants in polyamides 6 (PA6) and 6.6 (PA6.6). Polym Degrad Stab 2012: 97(12); 2503-2510.
15. Cusack P, Hornsby P. Zinc stannate-coated fillers: novel flame retardants and smoke suppressants for polymeric materials. J Vinyl Addit Technol 1999: 5(1); 21-30.
16. Horrocks AR, Smart G, Price D, Kandola BK. Zinc stannates as alternative synergists in selected flame retardant systems. J Fire Sci 2009: 27; 495-521.
17. Karrasch A, Wawrzyn E, Schartel B, Jager C. Solid-State NMR on thermal and fire residues of bisphenol A polycarbonate/silicone acrylate rubber/bisphenyol A bis (diphenyl-phosphate)/(PC/SiR/BDP) and PC/SiR/BDP/ZnB) – Part I: PC Charring and the impact of BDP and ZnB. Polym Degrad Stab 2010: 95; 2525-

2533.

18. Samyn F, Bourbigot S, Duquesne S, Delobel R. Effect of zinc borate on the thermal degradation of ammonium polyphosphate. Thermochim Acta 2007: 546; 134-144.
19. Pawlowski KH, Schartel B, Ficher MA Jager C. Flame retardancy mechanisms of bisphenol a bis (diphenyl phosphate) in combination with zinc borate in bisphenol a polycarbonate/acryolnitrile-butadiene-styrene blends. Thermochim Acta 2010: 498; 92-99.
20. Babushok V, Tsang W. Inhibitor rankings for alkane combustion. Comb Flame 2000: 123; 488-506.
21. Camino G, Costa L, Luda di Cortemiglia MP. Overview of fire retardant mechanisms. Polym Degrad Stab 1991:33; 131-154.
22. Kicko-Walczak E. Flame retarded halogenated unsaturated polyester resins. Thermal decomposition study. J Polym Eng 2003:23; 149-161
23. Bains RS, Cusack PA, Monk AW. A comparison of the fire retardant properties of zinc hydroxystannate and antimony trioxide in brominated polyester resins containing inorganic fillers. Eur Polym J 1990:26(11); 1221-1227
24. Horrocks AR, Smart G, Kandola B, Price D. Zinc stannate interactions with flame retardants in polyamides; Part 2: Potential synergies with non-halogen-containing flame retardants in polyamide 6 (PA6). Polym Degrad Stab 2012: 94(4); 645-652.
25. Aubert M, Wilen CE, Pfaendner R, Kniesel S, Hoppe H, Roth M. Bis(1-propyloxy-2,2,6,6-tetramethylpiperidin-4-yl)-diazene – An innovative multifunctional radical generator providing flame retardancy to polypropylene even after extended artificial weathering. Polym Degrad Stab 2011: 96; 328-333.
26. Zauner R, Jones A G. Scale-up of Continuous and Semibatch Precipitation Processes, Ind Eng Chem Res. 2000, 39, 2392-2403.
27. "PowDLL, a reusable .NET component for interconverting powder diffraction data: Recent developments", N. Kourkoumelis, ICDD Annual Spring Meetings, Ed. Lisa O'Neill, Powder Diffraction, 28, 2013, 137-48.
28. Holdsworth A. Novel metal complex fire retardants for engineering polymers. PhD thesis, University of Bolton, 2015
29. Kandola BK, Horrocks AR, Horrocks S. Evidence of interaction in flame-retardant fibre-intumescent combinations by thermal analytical techniques. Thermochim Acta 1997: 294; 113-125.
30. Zhao B, Chen L, Long JW, Chen HB, Wang YZ. Aluminum Hypophosphite versus alkyl-substituted phosphinate in Polyamide 6: Flame retardance, thermal degradation, and pyrolysis behavior. Ind Eng Chem Res 2013: 52(8); 2875-2886.
31. Costanzi S, Leonardi M. Polyester compositions flame retarded with halogen-free additives. US Pat. 7700680 B2, 2004.
32. Kohan MI. Nylon plastics. Cincinnati, USA: Hanser Gardner, 1995.
33. Anthrop DF, Searcy AW. Sublimation and thermodynamic properties of zinc oxide. J Phys Chem 1964: 68(8); 2335–2342.
34. Hubbard SA. Comparative toxicology of borates. Biol Trace Elem Res 1998: 66; 343-357.

35. Pike RD, Starnes, Jr. WH, Jeng JP , Bryant WS, Kourtesis P, Adams CW, Bunge SD, Kang YM, Kim AS, Kim JH, Macko JA, O'Brien CP. Low-valent metals as reductive cross-linking agents: A new strategy for smoke suppression of poly(vinyl chloride). Macromolecules 1997: 30(22); 6957-6965.
36. Heslop RB and Robinson PL. *Inorganic Chemistry, 2nd Edition*. London: Elsevier, 1963.
37. Zhang Z, Goodall JB, Brown S, Karlsson L, Clark RJ, Hutchinson JL, Rehman IU and Darr JA. Continuous hydrothermal synthesis of extensive 2D sodium titanate ($Na_2Ti_3O_7$) nano-sheets. Dalton Trans2010: 39(3); 711-14.
38. Weng X, Cockcroft JK, Hyett G, Vickers M, Boldrin P, Tang CC, Thompson SP, Parker JE, Knowles JC, Rehman I, Parkin I, Evans JRG and Darr JA. High-throughput continuous hydrothermal synthesis of an entire nanoceramic phase diagram. J Comb Chem 2009: 11(5); 829-834.

6: Acknowledgements

We would like to thank the EPSRC and William Blythe Ltd for their support (CASE Studentship), and additionally Drs G. J. Milnes and G. Smart, Mr A. Zarei and Mr S. Shafiee for their technical support. We would additionally like to thank William Blythe Ltd and Dr R. Pritchard and Mr. M. Jennings (University of Manchester) for their assistance and access to analytical equipment.

Tables

Table 1: Cations and anions selected for synthesis of 151 metal complex flame retardant candidates

Cations	Mg^{2+}, Al^{3+}, Ca^{2+}, Mn^{2+}, Fe^{2+}, Fe^{3+}, Cu^{2+}, Zn^{2+}, Sn^{2+}, Sn^{4+}
Metalloxyanions	$B(OH)_4^-$, CO_3^{2-}, $C_2O_4^{2-}$, HO^-, $Al(OH)_4^-$, $Si(OH)_4^-$, MoO_4^{2-}, $Sn(OH)_6^{2-}$, WO_4^{2-}
Phosphorus Oxyanions	$H_2PO_2^-$, HPO_3^-, PO_3^{2-}, PO_4^{3-}, $P_2O_7^{4-}$, $P_3O_{10}^{5-}$, $PhPO_3^{2-}$
Nitroxy Anions	o-$Ph(NO_2)O^-$, salicylaldoximate (sal^-), dimethylglyoximate (dmg^-), $Mn(NO_2)_6^{4-}$, $Cu(NO_2)_6^{4-}$, $Zn(NO_2)_6^{4-}$

Table 2: Summary of large scale syntheses

Target complex, A	Cation source, B	Cation source mass, C (g)	Cation source, D (mol)	Water, E (ml)	Anion source, F	Anion source mass, G (g)	Anion source, H (mol)	Water, I (ml)	Yield, J (%)	Notes
$FeAl_2(OH)_8$	$FeCl_2.4H_2O$	80.92	0.41	400	$NaAlO_2.2H_2O$	133.44	0.82	800	97.7	1
$Al_2(WO_4)_3$	$Al(NO_3)_3.9H_2O$	82.53	0.22	250	$Na_2WO_4.2H_2O$	108.85	0.33	250	97.0	
$ZnWO_4$	$ZnCl_2$	38.98	0.29	300	$Na_2WO_4.2H_2O$	94.34	0.29	300	91.2	
$SnWO_4$	$SnCl_2$	47.03	0.25	250	$Na_2WO_4.2H_2O$	81.80	0.25	250	94.0	
$Fe(H_2PO_2)_3$	$FeCl_3$	64.88	0.40	400	NaH_2PO_2	105.57	1.20	1200	85.9	2
$Sn(H_2PO_3)_2$	$SnCl_2$	68.26	0.36	400	NaH_2PO_3	73.82	0.72	700	c.a. 90	2
$SnPhPO_3$	$SnCl_2$	68.26	0.36	350	Na_2PhPO_3	72.74	0.36	350	c.a. 90	2
$Sn_5(P_3O_{10})_2$	$SnCl_2$	86.27	0.46	500	$Na_5P_3O_{10}$	66.95	0.18	400	N/A	3
Notes: 1 – Product was difficult to filter, 2 – Anions were prepared from free acids and stoichiometric amount of Na_2CO_3, 3 – Formed gelatinous precipitate that proved impossible to isolate.										

Table 3: Calcination conditions used for preparation of metal complexes for compounding

Compound	Formula	Calcination
Iron Aluminate	$FeAl_2O_4$	240 °C
Aluminium Tungstate	$Al_2(WO_4)_3$	240 °C
Zinc Tungstate	$ZnWO_4$	240 °C
Tin (II) Tungstate	$SnWO_4$	240 °C, vacuum
Iron (III) Hypophosphite	$Fe(H_2PO_2)_3$	80 °C
Tin (II) Hydrogenphosphite	$Sn(H_2PO_3)_2$	80 °C
Tin (II) Phenylphosphonate	$SnPhPO_3$	80 °C

Table 4: Small scale metal complex syntheses and respective cation:anion molar ratios

Cation / Anion	Formula	Mg^{2+}	Al^{3+}	Ca^{2+}	Mn^{2+}	Fe^{2+}	Fe^{3+}	Cu^{2+}	Zn^{2+}	Sn^{2+}	Sn^{4+}
Borate	$B(OH)_4^-$	1:2	1:3	1:2	1:2	1:2	1:3	1:2		1:2	1:4
Carbonate	CO_3^{2-}	1:1	2:3	1:1	1:1	1:1	2:3	1:1	1:1	1:1	1:2
Oxalate	$C_2O_4^{2-}$	1:1	2:3	1:1	1:1	1:1	2:3	1:1	1:1	1:1	1:2
Hydroxide	HO^-			1:2	1:2	1:2	1:3	1:2	1:2	1:2	1:4
Aluminate	$Al(OH)_4^-$	1:2	1:3	1:2	1:2	1:2	1:3	1:2	1:2	1:2	1:4
Silicate	SiO_3^{2-}	1:1	2:3	1:1	1:1	1:1	2:3	1:1	1:1	1:1	1:2
Molybdate	MoO_4^{2-}	1:1	2:3	1:1	1:1	1:1	2:3	1:1		1:1	1:2
Stannate	$Sn(OH)_6^{2-}$	1:1	2:3	1:1	1:1	1:1	2:3	1:1		1:1	1:2
Tungstate	WO_4^{2-}	1:1	2:3	1:1	1:1	1:1	2:3	1:1	1:1	1:1	1:2
P-Anions											
Hypophosphite	$H_2PO_2^-$	1:2		1:2	1:2	1:2	1:3	1:2	1:2	1:2	1:4
Hydrogen phosphite	$H_2PO_3^-$	1:2	1:3	1:2	1:2	1:2	1:3	1:2	1:2	1:2	1:4
Phosphite	HPO_3^-	1:1	2:3	1:1	1:1	1:1	2:3	1:1	1:1	1:1	1:2
Phosphate	PO_4^{3-}	3:2	1:1	3:2	3:2	3:2	1:1	3:2	3:2	3:2	3:4
Pyrophosphate	$P_2O_7^{4-}$	2:1	4:3	2:1	2:1	2:1	4:3	2:1	2:1	2:1	1:1
Triphosphate	$P_3O_{10}^{5-}$	5:2	5:3	5:2	5:2	5:2	5:3	5:2	5:2	5:2	5:3
Ph-phosphonate	$PhPO_3^-$	1:1	2:3	1:1	1:1	1:1	2:3	1:1	1:1	1:1	1:2
Nitroxy Anions											
o-Nitrophenol	$Ph(NO_2)O^-$	1:2	1:3	1:2	1:2	1:2	1:3	1:2	1:2	1:2	1:4
Salicylaldoxime	$Ph(OH)CNO^-$	1:1	1:1	1:1	1:1	1:1	1:1	1:1	1:1	1:1	1:1
dmg	$C_4H_7N_2O_2^-$	1:1	1:1	1:1	1:1	1:1	1:1	1:1	1:1	1:1	1:1
$Mn(NO_2)_6^{4-}$		2:1	4:3	2:1	2:1	2:1	4:3	2:1	2:1	2:1	1:1
$Cu(NO_2)_6^{4-}$		2:1	4:3	2:1	2:1	2:1	4:3	2:1	2:1	2:1	1:1
$Zn(NO_2)_6^{4-}$		2:1	4:3	2:1	2:1	2:1	4:3	2:1	2:1	2:1	1:1

Key: Red cells – not precipitated, blue cells – known FR compounds, green cells – same metal in cation and anion. Emboldened samples met the screening criteria i. to vi. outlined above. Italicized samples met the desired T_{580} level of 25% but failed to meet other criteria.

Table 5: Metal complex/PA66 thermal analytical T_{580} residue values.

Oxides	**Formula**	**Mg^{2+}**	**Al^{3+}**	**Ca^{2+}**	**Mn^{2+}**	**Fe^{2+}**	**Fe^{3+}**	**Cu^{2+}**	**Zn^{2+}**	**Sn^{2+}**	**Sn^{4+}**
Borate	$B(OH)_4^-$	11.7	15.1	18.7	24.2	14.2	14.6	14.5		24.4	16.7
Carbonate	CO_3^{2-}	15.7	16.4	22.8	8.7	18.2		16.6	15.5	**26.6**	**31.3**
Oxalate	$C_2O_4^{2-}$	3.3		19.1	8.0	10.6		11.0	10.7	11.1	
Hydroxide	HO^-				17.1	13.7	**25.3**	19.4	22.3	23.4	18.8
Aluminate	$Al(OH)_4^-$	19.3		16.9	18.3	**24.8**	19.1	21.1	18.8	21.6	20.5
Silicate	SiO_3^{2-}	13.3	21.2	17.3	16.0	13.6	14.9	20.2	14.2	24.9	**27.4**
Molybdate	MoO_4^{2-}		18.8	20.0	11.6	17.5	24.0	24.5		18.0	8.4
Stannate	$Sn(OH)_6^{2-}$	15.5	13.4	19.8	15.5	7.6	17.4	17.9			
Tungstate	WO_4^{2-}		**27.4**	16.8	24.1	13.0	23.7	22.4	**32.5**	**26.9**	22.0
P-Anions											
Hypophosphite	$H_2PO_2^-$						**40.7**				
Hydrogen phosphite	$H_2PO_3^-$				23.3		**25.5**			**34.2**	
Phosphite	HPO_3^-	20.0	17.0	22.8	17.6	19.5	**26.1**	**31.4**	**26.9**	**27.6**	
Phosphate	PO_4^{3-}	22.2	19.7	18.4	22.9	18.9	18.4	19.4	22.3	**27.7**	18.7
Pyrophosphate	$P_2O_7^{4-}$	19.3	18.3	20.2	16.9	18.4	19.2	22.4	23.1	23.5	
Triphosphate	$P_3O_{10}^{5-}$	24.9	18.3	22.3	23.8	23.3	23.2	24.3	23.1	**30.1**	
Ph-phosphonate	$PhPO_3^-$	12.9	19.8	14.5	12.8	15.0	19.5	14.8	12.9	**26.7**	21.3
Nitroxy Anions											
o-Nitrophenol	$Ph(NO_2)O^-$		9.0	10.1	1.2	10.5		10.1	**27.1**		13.1
Salicylaldoxime	$Ph(OH)CNO^-$	2.6		6.7	6.0	5.2		5.8	1.3		
dmg	$C_4H_7N_2O_2^-$	1.7	0.0		5.3	0.0	0.2	5.1	6.3	1.8	13.3
$Mn(NO_2)_6^{4-}$											16.7
$Cu(NO_2)_6^{4-}$											18.4
$Zn(NO_2)_6^{4-}$											**24.4**

Key: Colour coding as in Table 4, namely Red cells – not precipitated, blue cells – known FR compounds, green cells – same metal in cation and anion. Emboldened samples met the screening criteria i. to vi. outlined above. Italicized samples met the desired T_{580} level of 25% but failed to meet other criteria. Emboldened figures are for complexes exhibiting $T_{580} \geq 25\%$

Table 6: Thermal analytical data for the 19 selected salts

Metal Complex	Formula	T_{10}, °C	Maximum Mass Difference, %*	
			480-500 °C	540-560 °C
PA66 control	-	409	-	-
Tin(II) carbonate/oxide	$SnCO_3 \rightarrow SnO$	370	19	13
Tin(IV) carbonate/oxide	$Sn(CO_3)_2 \rightarrow SnO_2$	377	12	14
Iron(III) hydroxide	$Fe(OH)_3 \rightarrow FeOOH$	375	8	7
Iron(II) aluminate	$Fe(Al(OH_4)_2)$	372	8	8
Tin(IV) silicate	$Sn(SiO_2)_2.4H_2O$	404	8	11
Aluminium tungstate	$Al_2(WO_4)_3.6H_2O$	411	7	9
Zinc tungstate	$ZnWO_4.2H_2O$	384	9	14
Tin(II) tungstate	$SnWO_4.2H_2O$	364	10	13
Iron(III) hypophosphite	$Fe(H_2PO_2)_3$	362	16	16
Iron(III) hydrogen phosphite	$Fe(H_2PO_3)_3$	378	7	9
Tin(II) hydrogen phosphite	$Sn(H_2PO_3)_2$	393	13	17
Iron(III) phosphite	$Fe(HPO_3)_3$	375	11	7
Copper phosphite	$Cu(HPO_3)_2$	330	9	15
Zinc phosphite	$Zn(HPO_3)_2$	389	7	10
Tin(II) phosphite	$Sn(HPO_3)_2$	397	7	10
Tin(II) phosphate	$Sn_3(PO_4)_3$	356	8	10
Tin(II) triphosphate	$Sn_5(P_3O_{10})_2$	396	11	14
Tin(II) phenyl phosphonate	$SnPhPO_3$	372	17	16
Tin(IV) hexanitrozincate	$Sn(Zn(NO_2)_6)$	397	5	7
Note: *Values are quoted as highest levels in each temperature range.				

Table 7: Fire performance data for the 8 selected, larger synthetic scale compounds in PA66.

Sample	**[FR]**	**TGA/DTA (Air)**				**TGA/DTA (N_2)**				**UL94 specimen ratings**			**LOI,**	**Cone calorimetric data**						
	wt%	T_5 °C	DTG_{max}, °C	M_{500}, wt%	M_{580}, wt%	T_5, °C	DTG_{max}, °C	M_{500} wt%	M_{580} wt%	1	2	3	**vol%**	T_{ig}, s	T_{fo}, s	T_{PHRR}, s	PHRR, kW/m^2	R_{PHRR},%	THR, MJ	R_{THR},%
PA66	-	386	461	11.2	3.9	402	453	3.8	3.5	V-2	F	F	22.9	50	142	104	1625	-	84.2	-
$Fe(AlO_2)_2$	5	351	416	10.4	2.2	360	410	5.6	5.3	V-2	F	F	23.7	32	135	80	899	45	69.2	18
$Al_2(WO_4)_3$	5	368	437	14.0	7.8	369	494	6.5	6.0	V-0	V-2	F	23.0	35	146	110	1156	29	79.3	6
$ZnWO_4$	5	349	387	9.6	4.1	360	428	4.9	4.6	F	F	F	21.5	38	138	110	1190	27	72.4	14
$SnWO_4$	5	368	442	14.3	3.6	371	432	6.0	5.6	V-2	F	F	22.0	26	134	85	954	41	71.8	15
$Fe(H_2PO_2)_3$	5	366	449	14.5	6.0	374	415	4.8	4.5	V-2	F	F	22.7	-	-	-	-	-	-	-
$Sn(HPO_3)_2$	5	385	452	14.5	7.8	382	441	6.5	6.1	F	F	F	20.7	41	157	93	891	45	57.3	32
	10	379	457	19.5	12.1	372	442	9.6	9.3	F	F	F	21.8	41	152	75	831	0.511	66.3	21
$SnPhPO_3$	5	359	438	15.5	6.7	382	382	6.5	6.1	V-2	F	F	21.8	27	108	78	1043	35	75.5	10
	10	367	420	18.2	11.7	366	426	8.2	7.0	F	F	F	22.8	45	168	93	829	49	73.7	12

Key: DTG_{max} is the DTG maximum temperature, M_{500} and M_{580} are the percentage residues at 500 and 589 °C respectively, percentage reductions (±1%) in PHRR and THR respectively are R_{PHRR} (= (1-($PHRR_{PA66+MC}$/$PHRR_{PA66}$))x100) and R_{THR} (= (1-($THR_{PA66+MC}$/THR_{PA66}))x100)

Figures

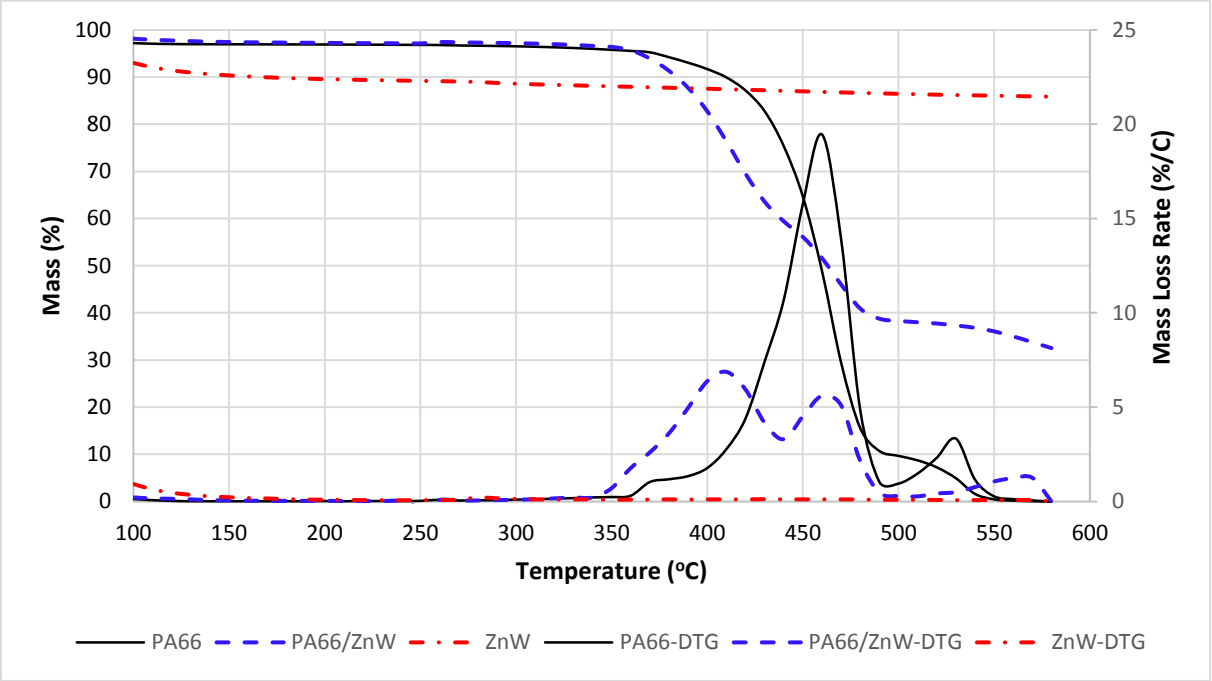

Figure 1: TGA and DTG responses at 20 °C/min in air of PA66, $ZnWO_4$ and PA66/$ZnWO_4$ (3:1) mixture.

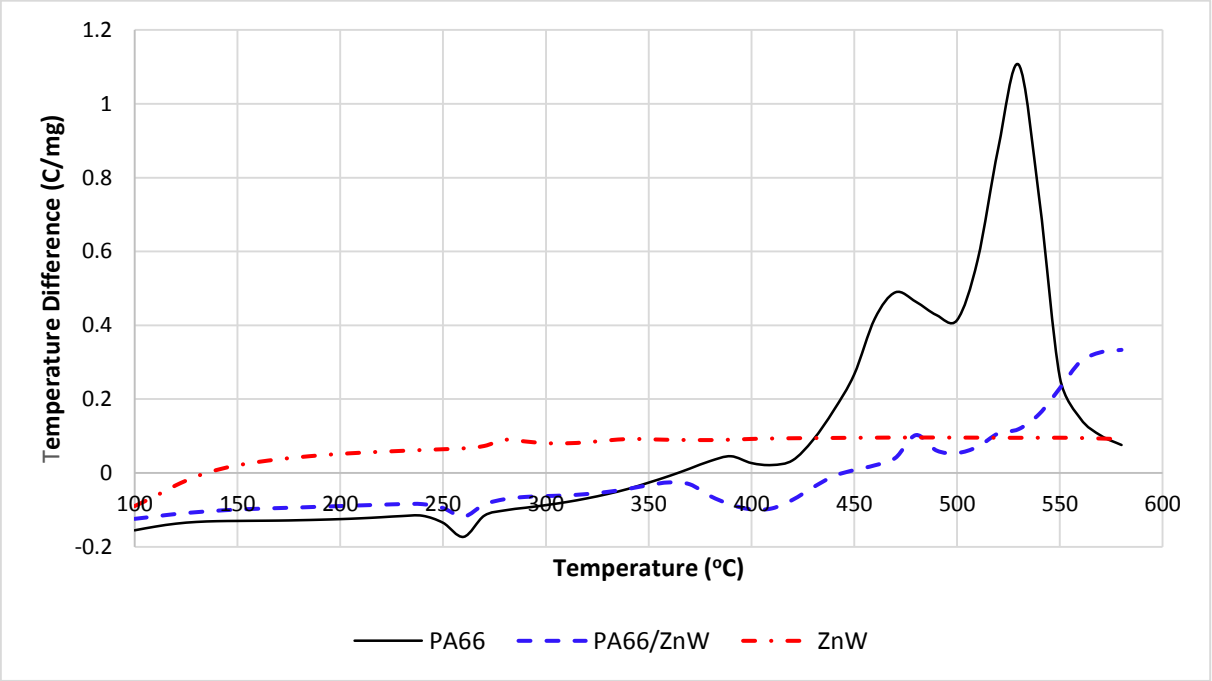

Figure 2: DTA responses at 20 °C/min in air of PA66, $ZnWO_4$ and PA66/$ZnWO_4$ powder mix (1:3).

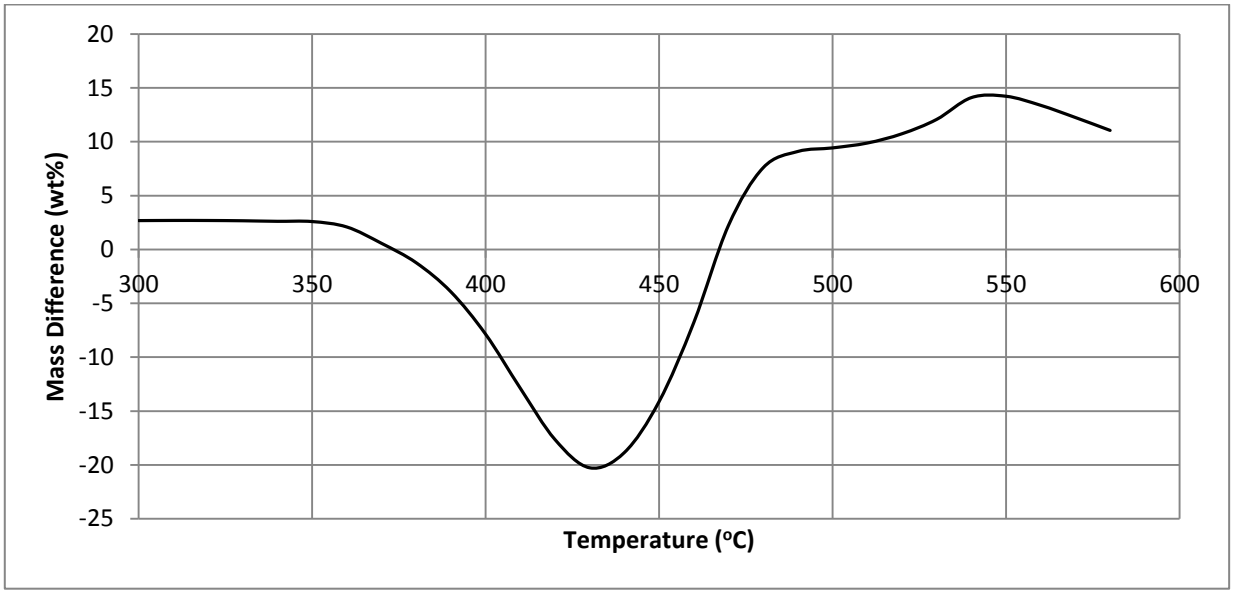

Figure 3: Differential mass TGA graph between the observed and calculated TGA degradation curves of the 3:1 mix of PA66 and $ZnWO_4$ powders under air.

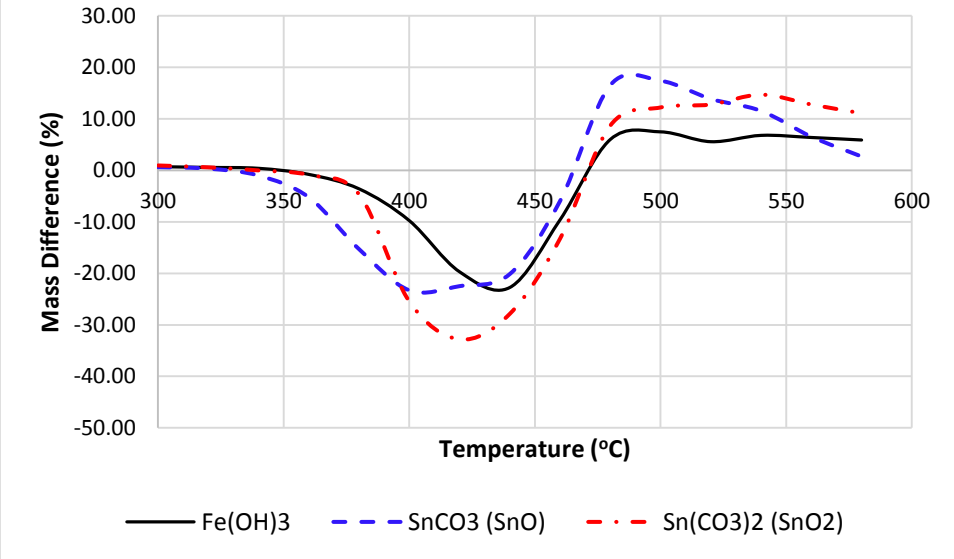

Figure 4. Differential mass TGA graphs for tin (II) and (IV) carbonates/oxides and Fe (III) hydroxide under air.

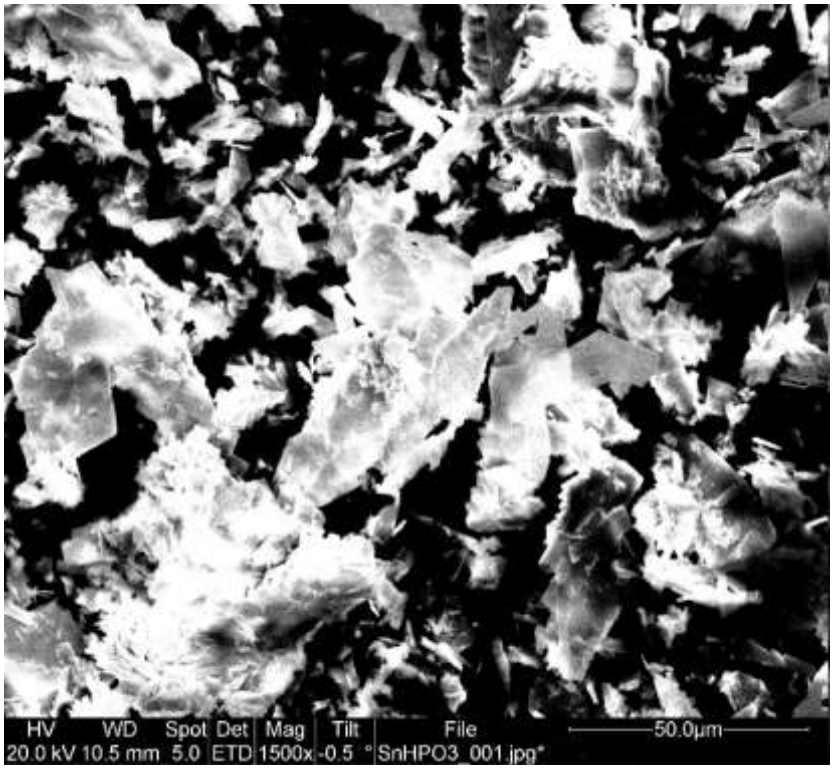

Figure 5: SEM image of $SnHPO_3$ platelets.

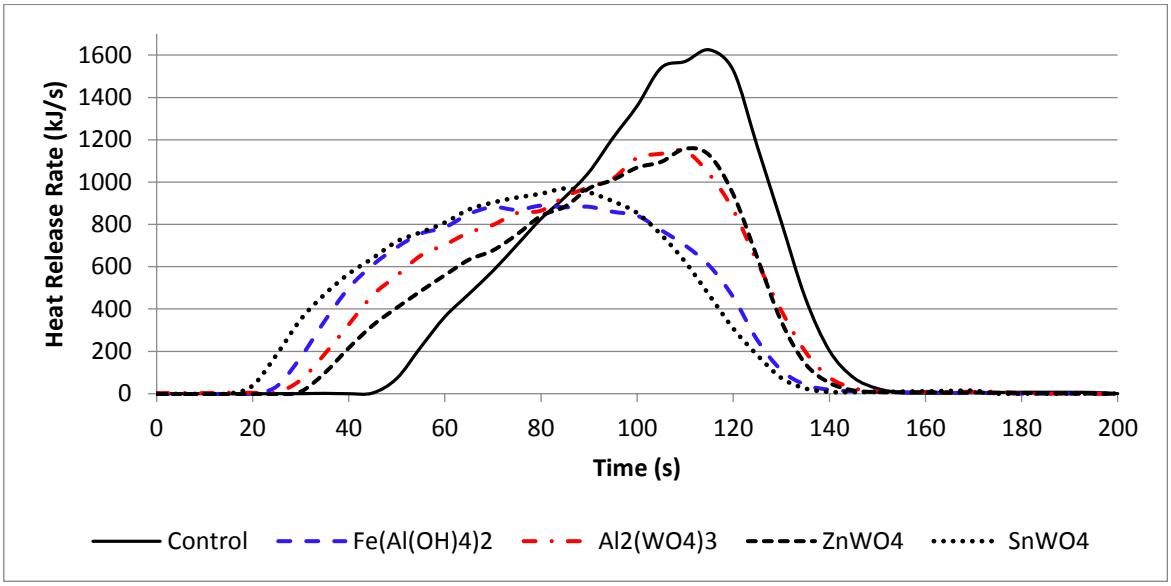

(a)

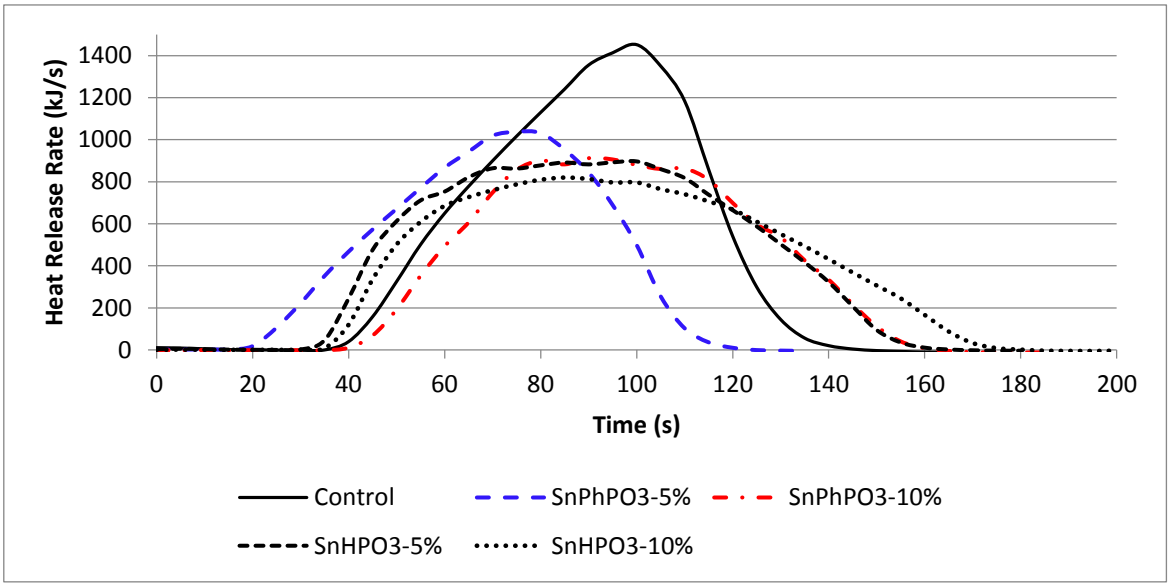

(b)

Figure 6: Cone calorimetric heat release data for PA66 containing (a) 5 wt% of iron aluminate and aluminium, zinc and tin (II) tungstates, and (b)5 and 10 wt% of tin (II) phosphite and phenylphosphonate.

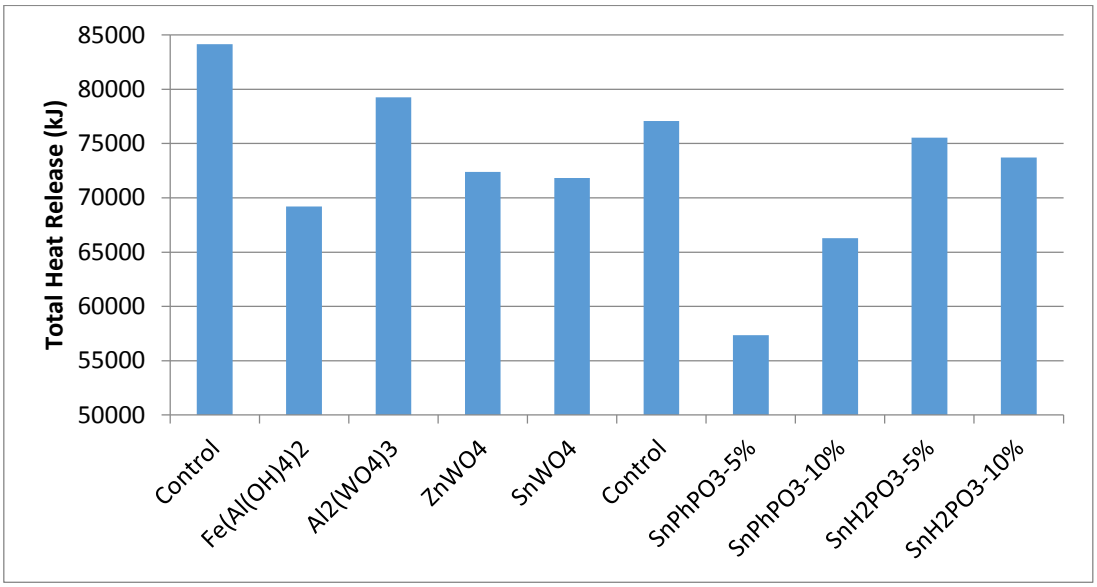

Figure 7: Cone calorimetry total heat release values of PA66 containing 5 or 10 wt% of metal complexes

Supplementary Tables

Table S1: Exemplar calculations of differential mass curve for $ZnWO_4$ based on the raw TGA data. PA66, ZnW and Exp are the TGA responses for pure PA66, ZnW and the combined 3:1 PA66:ZnW powder mixture respectively.

	TGA original percentage mass values				
Temp, °C	PA66	ZnW	Calc	Exp	Diff. mass, %
300	96.48996	88.6	94.51747	97.2	2.682532
310	96.39285	88.47	94.41214	97.11	2.697862
320	96.27632	88.36	94.29724	96.99	2.692759
330	96.13066	88.26	94.16299	96.83	2.667005
340	95.95587	88.15	94.0044	96.62	2.6156
350	95.74223	88.04	93.81667	96.41	2.593328
360	95.50917	87.95	93.61938	95.71	2.090621
370	95.20814	87.85	93.3686	93.94	0.571396
380	94.1788	87.75	92.5716	91.34	-1.2316
390	93.0038	87.64	91.66285	87.73	-3.93285
400	91.66371	87.54	90.63278	82.77	-7.86278
410	89.89635	87.43	89.27977	76.4	-12.8798
420	87.12879	87.32	87.17659	69.53	-17.6466
430	82.73953	87.21	83.85715	63.59	-20.2671
440	75.33022	87.09	78.27017	59.42	-18.8502
450	64.6581	86.98	70.23857	56.12	-14.1186
460	48.89754	86.87	58.39066	51.61	-6.78066
470	29.4469	86.76	43.77517	46.01	2.234827
480	15.54109	86.65	33.31832	40.91	7.591679
490	10.69446	86.55	29.65834	38.76	9.101658
500	9.657347	86.46	28.85801	38.29	9.43199
510	8.713462	86.37	28.1276	38.01	9.882404
520	7.234513	86.28	26.99589	37.74	10.74411
530	4.924324	86.2	25.24324	37.32	12.07676
540	1.594506	86.13	22.72838	36.83	14.10162
550	0.438926	86.06	21.84419	36.07	14.22581
560	0.168967	85.99	21.62423	35.01	13.38577
570	0.048554	85.92	21.51642	33.77	12.25358
580	0	85.85	21.4625	32.52	11.0575

Table S2: Summary of Characterisation Data for Metal Complexes [28]

Compound	Theoretical	XRF	AA	ICP	Titr	Grav	XRF (Rat)	XRD	TGA	PSD (10/50/90)	FTIR	Na^+	Cl^-
$FeAl_2O_4$	(Fe) 30.7	41.8	34.8	24.3		-		M[1]	-	0.7/2.7/8.0	M[2]	0.1	0.7
	(Al) 29.7	-	29.4	29.6		-		-	-	-	-	-	-
	(H_2O) 27	-	-	-		-		-	23	-	-	-	-
$ZnMoO_4$	(Zn) 29.0			21.7				M[3]	-	1.3/5.0/14.7	Y[4,5]	-	0.1
	(Mo) 42.6			33.2				-	-	-	-	-	-
	(H_2O) 14			-				-	7	-	-		-
$Al_2(WO_4)_3$	(Al) 6.8		10.2	2.5				Y	-	0.6/1.9/6.5	N/R	0.3	-
	(W) 69.1			-		69.4		-	-	-	-	-	-
	(H_2O)	12		-				-	11	-	-	-	-
$ZnWO_4$	(Zn) 20.9		12.9	17.6			(1:2.81)	Y	-	0.5/1.4/4.7	Y[6, 7]	0.3	0.2
	(W) 58.7			-		55.5	1:2.98	-	-	-	-	-	-
	(H_2O)	10		-				-	5	-	-	-	-
$SnWO_4$	(Sn) 32.4		36.9	28.7			(1:1.55)	Y	-	0.5/1.1/3.5	Y[8]	0.2	0.3
	(W) 50.1			-		53.7	1:1.55	-	-	-	-	-	-
	(H_2O)	9		-				-	2	-	-	-	-
$Fe(H_2PO_2)_3$	(Fe) 22.3	21.4	22.7	22.1	-			Y	-	-	Y[9]	-	-
	(P) 37.0			37.0	-			-	-	-	-	-	-
$Sn(H_2PO_3)_2$	(Sn) 42.3	42.4		42.7	41.7[10]			-	-	2.7/12.0/30.2	N/R	-	0.0
	(P) 22.1			-	-			-	-	-	-	-	-
$SnPhPO_3$	(Sn) 43.2			[11]	41.1			-	-	1.3/4.5/19.3	Y[12]	-	1.5
	(P) 11.3			-	-			-	-	-	-	-	-

Key, Notes and References: Y: Matches reference, M: Multiphasic, N: No usable spectra obtained, N/R: No reference available for comparison.
Titr: Sn oxidation titration result.
Grav: tungsten gravimetric result.
All values except PSD (µm) are expressed as wt% of total.
Superscripts: 1: Mix of Fe_xO_y and $Al(OH)_3$, 2: S. Sivakumar et. al, *Spectrochim. Acta. A: Mol. Biolmol. Spec.*, 128, 2014, 69-75. 3: $NaZnMoO_4OH$, 4: Y. Keereeta, T. Thongtem and S. Thongtem, *Superlattices and Microstructures*, 69, 2014, 253-264, 5: T. Chengaiah, C. K. Jayasankar, K. Pavani and L. Rama Moorthy, *Optics Communications*, 312, 2014, 233-237, 6: *Mat. Sci. and Eng.*, 177, 2012, 19, 645-651, 7: *Mat. Sci. and Eng.*, 164, 2009, 1, 16-22, 8: R. Huang, H. Ge, X. Lin, Y. Guo, R. Yuan, X. Fu and Z. Li, *RSC Advances*, 4, 2013, 9: Manufacturer reference spectrum; 10: Divided observed result by 1.5 to account for oxidation of anion; 11: Gives erroneous and variable results; 12: Manufacturer reference spectrum of starting phosphonic acid.

Supplementary Figures

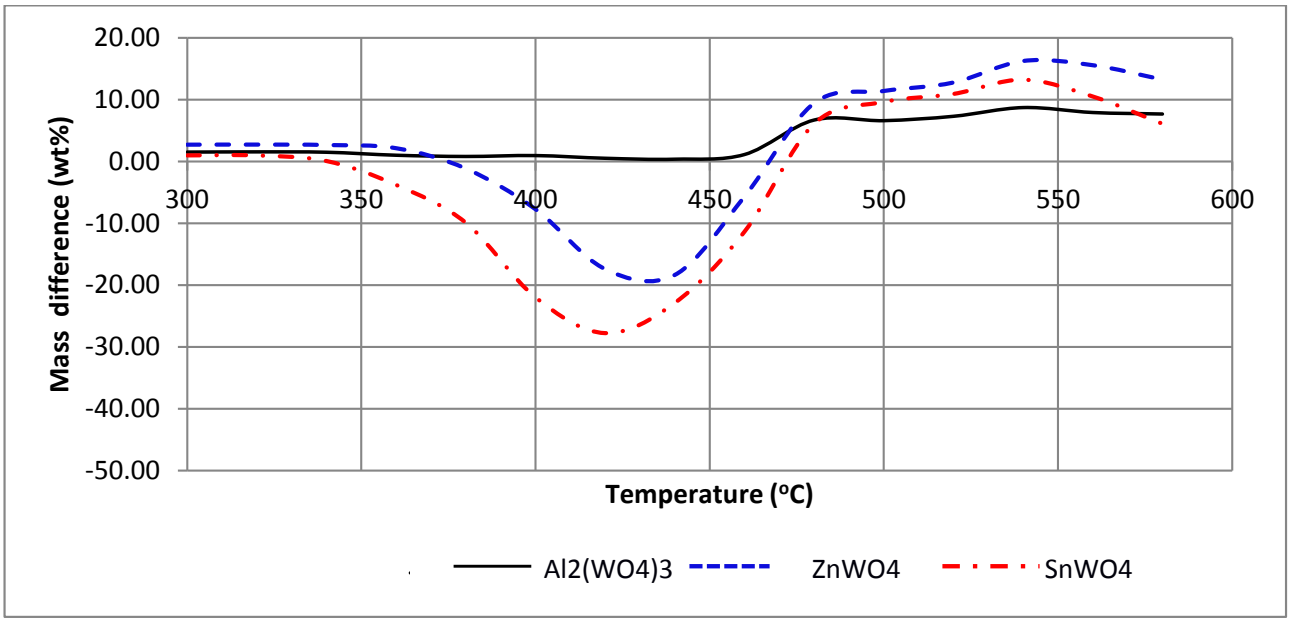

Figure S1: Differential mass TGA graphs for the aluminium, zinc and tin (II) tungstate samples under air

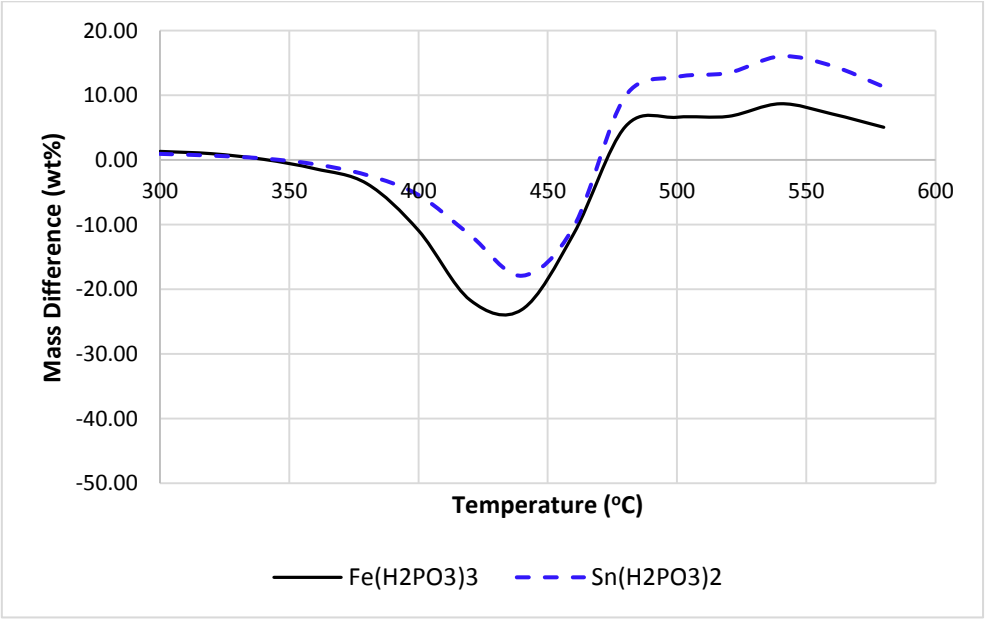

Figure S2: Differential mass TGA graphs for the iron (III) and tin (II) hydrogen phosphite samples under air

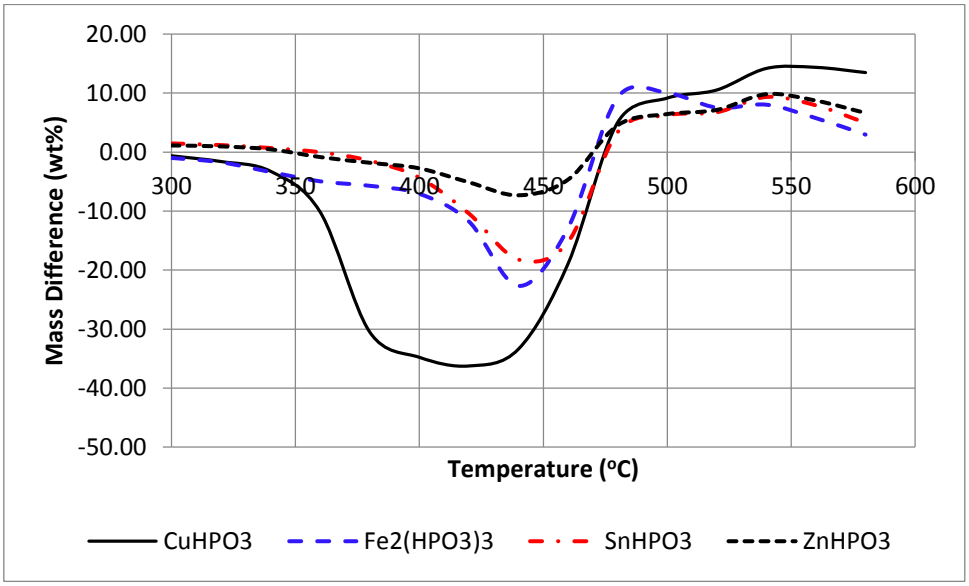

Figure S3: Differential mass TGA graphs for the selected phosphite samples under air.

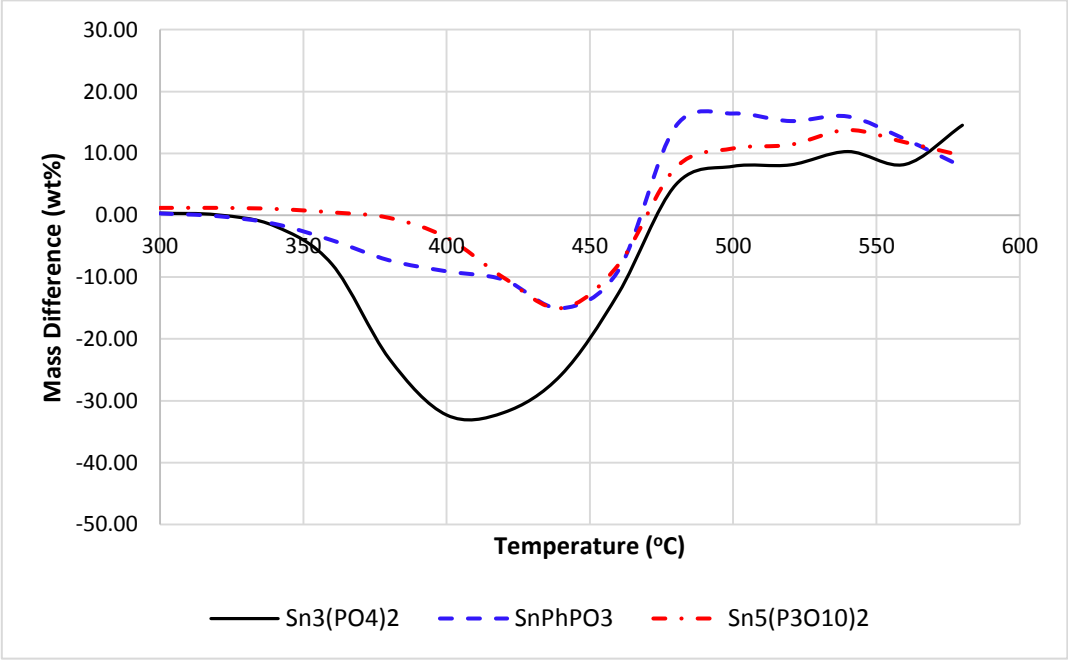

Figure S4: Differential mass TGA graphs for the selected phosphorus-containing samples under air.

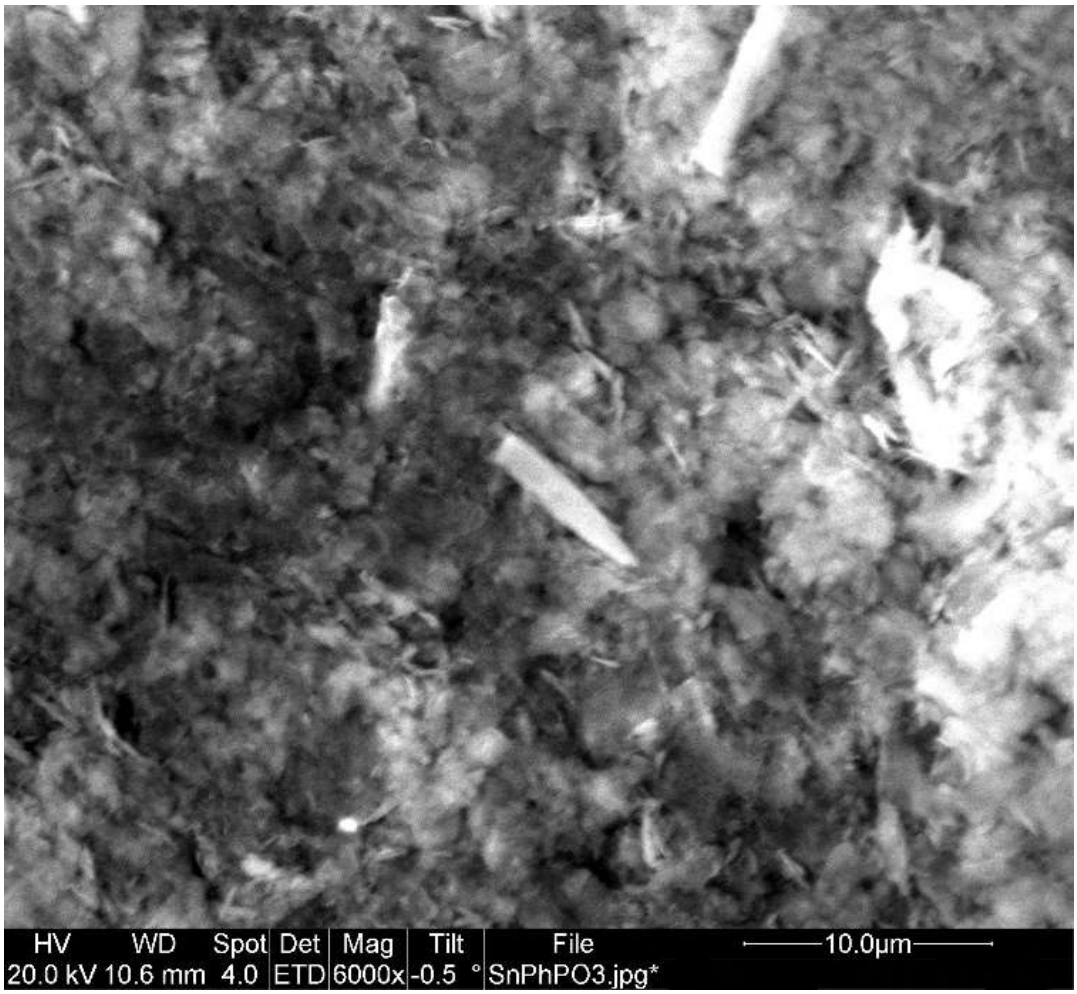

Figure S5: SEM image of $SnPhPO_3$ platelets.

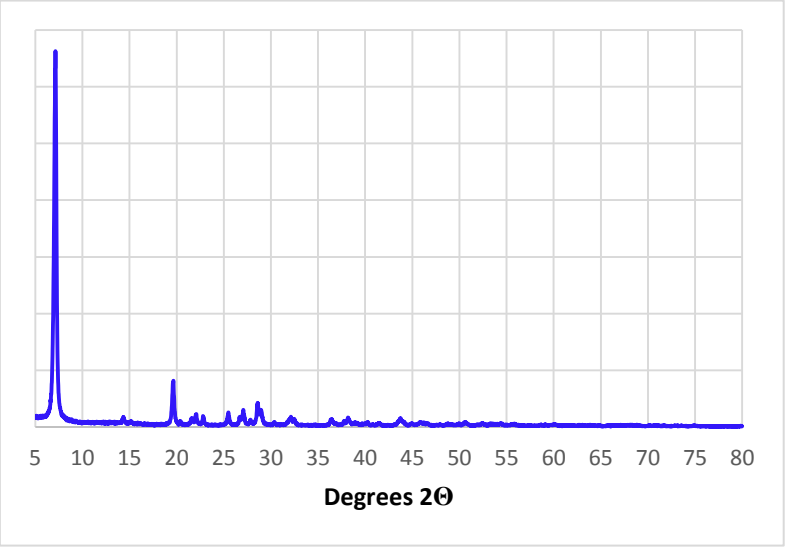

Figure S6: XRD pattern of $SnPhPO_3$.